Revision of *'Balaena' belgica* reveals a new right whale species, the possible ancestry of the northern right whale, *Eubalaena glacialis*, and the ages of divergence for the living right whale species

Michelangelo Bisconti Corresp., 1 , **Olivier Lambert** 2 , **Mark Bosselaers** 2, 3

1 San Diego Natural History Museum, San Diego, U.S.A.

2 Royal Belgian Institute of Natural Sciences, Brussels, Belgium

3 Zeeland Royal Society of Sciences, Middelburg, The Netherlands

Corresponding Author: Michelangelo Bisconti
Email address: michelangelobisconti@gmail.com

In 1941, O. Abel established *Balaena belgica* based on a series of fused cervical vertebrae and citing other cranial fragments from the late Neogene of the Antwerp harbor (northern Belgium). Later, Plisnier-Ladame and Quinet (1969) added a neurocranium and other skeletal remains from the same area to this species. Recently, the neurocranium was re-assigned to the genus *Eubalaena* thanks to newer phylogenetic analyses. Here, a new description is provided of materials previously assigned to *'Balaena' belgica* together with taxonomic revisions. Our work suggests that the cervical complex originally designated as the type of *'Balaena' belgica* is too poorly preserved to be used as such and is assigned to Balaenidae gen. et sp. indet., thus making *'Balaena' belgica* a nomen dubium. In addition to the neurocranium, the other remains consist in a fragment of maxilla assigned to Balaenidae gen. et sp. indet. and in a humerus assigned to *Eubalaena* sp. Discovered in the Kruisschans Sands Member of the Lillo Formation (3.2-2.8 Ma, Piacenzian, Late Pliocene), the neurocranium is designated as the holotype of the new species *Eubalaena ianitrix*. Our phylogenetic analysis supports a sister-group relationship of *E. ianitrix* and *E. glacialis*, and helps constraining the ages of origin for balaenid clades. Ecological and phylogenetic data suggest that *E. ianitrix* may represent the direct ancestor of *E. glacialis*, the latter having evolved through phyletic transformation including body size increase during the temperature decline of the Late Pliocene.

1 **Revision of *'Balaena' belgica* reveals a new right whale species, the possible**

2 **ancestry of the northern right whale, *Eubalaena glacialis*, and the ages of**

3 **divergence for the living right whale species**

5 Michelangelo Bisconti,[1] Olivier Lambert[2] and Mark Bosselaers[2,3]

7 [1]San Diego Natural History Museum, Balboa Park, 1788 El Prado, San Diego, CA 92101, USA

8 [2]Royal Belgian Institute of Natural Sciences, Rue Vautier 29, 1000 Brussels, Belgium

9 [3]Zeeland Royal Society of Sciences, Middelburg, The Netherlands

11 Corresponding Author

12 Michelangelo Bisconti

13 Email address: michelangelobisconti@gmail.com

15 **ABSTRACT**

16 In 1941, O. Abel established *Balaena belgica* based on a series of fused cervical vertebrae and

17 citing other cranial fragments from the late Neogene of the Antwerp harbor (northern Belgium).

18 Later, Plisnier-Ladame and Quinet (1969) added a neurocranium and other skeletal remains from

19 the same area to this species. Recently, the neurocranium was re-assigned to the genus *Eubalaena*

20 thanks to newer phylogenetic analyses. Here, a new description is provided of materials previously

21 assigned to *'Balaena' belgica* together with taxonomic revisions. Our work suggests that the

22 cervical complex originally designated as the type of *'Balaena' belgica* is too poorly preserved to

23 be used as such and is assigned to Balaenidae gen. et sp. indet., thus making *'Balaena' belgica* a

24 nomen dubium. In addition to the neurocranium, the other remains consist in a fragment of maxilla

25 assigned to Balaenidae gen. et sp. indet. and in a humerus assigned to *Eubalaena* sp. Discovered

26 in the Kruisschans Sands Member of the Lillo Formation (3.2-2.8 Ma, Piacenzian, Late Pliocene),

27 the neurocranium is designated as the holotype of the new species *Eubalaena ianitrix*. Our

28 phylogenetic analysis supports a sister-group relationship of *E. ianitrix* and *E. glacialis*, and helps

29 constraining the ages of origin for balaenid clades. Ecological and phylogenetic data suggest that

30 *E. ianitrix* may represent the direct ancestor of *E. glacialis*, the latter having evolved through

31 phyletic transformation including body size increase during the temperature decline of the Late

32 Pliocene.

Introduction

37   Living right whales include North Atlantic, southern and North Pacific right whales, all of them

38   grouped within the genus *Eubalaena* (Cetacea, Mysticeti, Balaenidae; Kenney, 2009; Rice, 2009).

39   The North Atlantic or northern right whale obviously inhabits the North Atlantic ocean, the

40   southern right whale is distributed in the waters around Antarctica, and the North Pacific right

41   whale is present in a portion of the Pacific that is limited in the south by southern Japan and the

42   southern portion of the California peninsula (Kenney, 2009). Recent studies have addressed

43   molecular taxonomy, population dynamics, and distribution patterns of these whales suggesting

44   that the genus *Eubalena* should include three species corresponding to the three groups mentioned

45   above (namely, *Eubalaena glacialis*, *E. australis* and *E. japonica*) (e.g., Rosenbaum et al., 2000).

46   Although a full agreement on this point has not been reached yet, it is largely acknowledged that

47   North Atlantic and North Pacific right whales are suffering high extinction risk (e.g., Clapham et

48   al., 1999). This is probably due to the catastrophic bottleneck effect induced into their populations

49   by human hunting activities during 19th and 20th centuries (e.g., Gaskin, 1986) that drastically

50   reduced the size of their populations in a brief period.

51   The assessment of the genetic diversity of the living right whale populations largely depends on

52   the reconstruction of the population size before the start of industrial whaling (Rooney et al., 2001;

53   Rosenbaum et al., 2000, Malik et al., 2000). Such a reconstruction depends on several factors

54   including the phylogenetic history of the genus and divergence time from the living species that is

55   phylogenetically closest to the living right whales (Rooney et al., 2001), namely the bowhead

56   whale *Balaena mysticetus*. The study of the fossil record may help determining the antiquity of the

57   genus *Eubalaena* and constraining the time of divergence of *Eubalaena* from the bowhead whale

58   (McLeod et al., 1993; Santangelo et al., 2005).

59   The fossil record of *Eubalaena* is scanty and scattered around the northern hemisphere. A right

60   whale skull from the Pleistocene of Japan was described by Nishiwaki & Hasegawa (1969) and

61   reviewed by Kimura (2009). Kimura (2009) also described *Eubalaena shinshuensis* from the latest

62   Miocene of the Gonda Formation, Nagano Prefecture, Japan. A partial skull of an indeterminate

63   species of *Eubalaena* was described by Bisconti (2002) from the Upper Pliocene of Tuscany,

64   Central Italy. Fragmentary tympanic bullae assigned to *Eubalaena* spp. were described by Morgan

65   (1994) from the Nashua Formation in Florida (latest Pliocene and earliest Pleistocene) and

66   Boessenecker (2013) from the Purisima Formation in Central California (Late Pliocene). Finally,

67   Field et al. (2017) described a fragmentary skull assigned to *Eubalaena* sp. from the Tjorres

68   Formation in Island (Early Pliocene).

69   A large-sized balaenid skull from the "Merxemien" of Antwerp, northern Belgium, was described

70   by Plisnier-Ladame & Quinet (1969) who assigned it to *Balaena belgica*, a taxon established by

71   Abel (1941) based on a described and illustrated cervical complex and the mention of other cranial

72   remains. Bisconti (2003) questioned Abel's taxonomic decision and suggested that the skull should

73   be assigned to *Eubalaena*, a proposal supported by later phylogenetic analyses placing *'B.' belgica*

74   as sister-group to *E. glacialis* (Bisconti, 2005a; Churchill et al., 2012) or as sister-group to the

75   extant *Eubalaena* species (Marx & Fordyce 2015). However, a formal re-description of the

76   specimen is currently necessary to make sound taxonomic decisions.

77   The specimens previously assigned to *'Balaena' belgica* consist of:

78   (1) a cervical vertebrae complex discovered on March 6th, 1914 by G. Hasse in the docks of

79   the Antwerp harbor, figured by Abel (1941, pl. 2, fig. 9) and Plisnier-Ladame & Quinet

80   (1969, fig. 1, pls. 1 and 2), and bearings the inventory number of the Royal Belgian Institute

81   of Natural Sciences, Brussels (hereinafter RBINS) RBINS M. 881 (IG 8444);

82   (2) a partial neurocranium (RBINS M. 879a-f, IG 8652) discovered in 1921 in Oorderen (a

83   part of the Antwerp harbor) during the excavation of the first Kruisschans lock (Figs. 1 and

84   2), figured by Plisnier-Ladame & Quinet (1969, pls. 1-2);

85   (3) a large fragment of right maxilla (RBINS M. 880a-c, IG 8652) also discovered in 1921 in

86   Oorderen during the excavation of the first Kruisschans lock seemingly misidentified as a

87   fragment of mandible by Plisnier-Ladame & Quinet (1969), but never described or figured;

88   (4) a large isolated left humerus (RBINS M. 2280) without any locality data, most likely

89   corresponding to the specimen mentioned by Plisnier-Ladame & Quinet (1969), but never

90   described or figured.

91   In this paper, the material previously assigned to *'Balaena' belgica* Abel, 1941 is newly described

92   and compared with an extended sample of right, bowhead and pygmy right whales to get a

93   comprehensive analysis of anatomy and clear taxonomic assignments. The morphological

94   characters of the skull are then used in a new phylogenetic analysis of living and fossil right and

95   bowhead whales to (1) reveal the timing of the origin of the genus *Eubalaena* and the divergence

96   time from its closest living relative *Balaena mysticetus*, and (2) investigate whether the three living

97   right whale populations correspond to three different species confirming or not the results of

98   molecular analyses. Our results will hopefully provide molecular ecologists with useful

99   information for safer reconstructions of past population dynamics of these highly endangered

100   species.

101

102   **Materials and methods**

103 *Institutional abbreviations*

104 AMNH, American Museum of Natural History, New York, USA. IZIKO, IZIKO Natural History

105 Museum, Cape Town, South Africa. MSNT, Museo di Storia Naturale e del Territorio, Università

106 di Pisa, Calci, Italia. NBC, Naturalis Biodiversity Center, Leiden, The Netherlands. RBINS, Royal

107 Belgian Institute of Natural Sciences, Brussels, Belgium. Additional abbreviations are provided in

108 the Supplementary Information file.

109

110 *New species name*

111 The electronic version of this article in Portable Document Format (PDF) will represent a

112 published work according to the International Commission on Zoological Nomenclature (ICZN),

113 and hence the new names contained in the electronic version are effectively published under that

114 Code from the electronic edition alone. This published work and the nomenclatural acts it contains

115 have been registered in ZooBank, the online registration system for the ICZN. The ZooBank

116 LSIDs (Life Science Identifiers) can be resolved and the associated information viewed through

117 any standard web browser by appending the LSID to the prefix http://zoobank.org/. The LSID for

118 this publication is: urn:lsid:zoobank.org:pub:C8D3FE95-303E-4EF4-86DD-1B453E124981. The

119 online version of this work is archived and available from the following digital repositories: PeerJ,

120 PubMed Central and CLOCKSS.

121

122 *Anatomy*

123 Anatomical terms for skull osteology follow Mead and Fordyce (2009); terminology for humerus

124 and cervical vertebrae follows Schaller (1999).

125

126   *Comparative analyses*

127   Comparative analyses were made with an extended balaenoid sample including specimens from

128   museums MSNT, RBINS, AMNH, NBC and IZIKO (specimens are listed in Bisconti, 2011). In

129   addition, specimens described in literature were used to complement first-hand observations (True,

130   1904; Omura, 1958; Tomilin, 1967; Tsai & Fordyce, 2015).

131

132   *Body size estimate*

133   Three methods for body size estimate were followed. First, we used the regression equation

134   provided by Pyenson & Sponberg (2011) that allows the reconstruction of the total body length

135   based on a measure of the bizygomatic width of the skull. The equation is the following (data in

136   mm):

137         $(1) \log(total\ body\ length) = 0.92(\log(bizygomatic\ width) - 1.64) + 2.67$

138   Pyenson & Sponberg (2011) used this equation to reconstruct total body lengths of living and fossil

139   cetaceans including mysticetes. Unfortunately, their study did not involve balaenid specimens,

140   therefore we cannot be sure that the equation (1) is well suited to provide an accurate reconstruction

141   of the total body length for Balaenidae. Moreover, results from equation (1) deviated from

142   observed values of intact specimens for amounts ranging from 47 to 37%. Bearing this in mind,

143   we corrected results generated by the equation (1) by reducing our results by 47 and 37%; in so

144   doing, we got two results from equation (1) corresponding to the range of estimates for the total

145   body length of RBINS M. 879a-f.

146   The second method used the occipital breadth as principal predictor as from the following

147   equation, provided by Evans et al. (2012) (measurements in mm):

148         $(2)\ body\ mass = 4.924 * 10^{-6}(occipital\ breadth)^{3.858}$

149   The equation (2) showed a high correlation coefficient in mammals ($R^2 = 0.9447$). Once a body

150   mass estimate was obtained, we used equation (3) to obtain an estimate of skeletal length. Equation

151   (3) is the following, as developed by Silva & Downing (1995):

152   $$(3)\ \log(body\ mass) = 3.08(\log(skeletal\ length)) - 4.84$$

153   This equation was extensively used in the reconstructions of body masses and skeletal lengths of

154   living and fossil mammals in previously published papers. Unfortunately, in marine mammals,

155   body mass may change during the life cycle depending on different patterns of activity performed

156   in the year (e.g., foraging, migration, female lactation etc.) thus the body mass estimate provided

157   by equation (3) is to be intended as mean body mass for a whale of a given length (Churchill et al.

158   2014).

159   Unfortunately, none of these equations was tested on balaenid records and it is not known if they

160   are actually able to retrieve correct results in this family. For this reason, we used also the

161   regression equation provided by Bisconti (2002) to predict the total skull length of a balaenid whale

162   based on supraoccipital length. The equation is the following:

163   $$(4)\ supraoccipital\ length = 0.3937(skull\ length) - 62.803$$

164   In this equation, skull length corresponds to condylobasal length. Unfortunately, the correlation

165   coefficient associated to this equation is rather low ($R^2 = 0.5967$) because the regression equation

166   is based on a limited and scattered dataset. Once a condylobasal length is obtained, we inferred the

167   total body length by tripling or quadrupling the condylobasal length. In fact, following Tomilin

168   (1967), the skull length is about 25-to-30% of the total body length in extant Balaenidae. Presently

169   it is not possible to be sure that this proportion applies to fossil balaenids; however, given that

170   skull and body sizes have important adaptive functions in Balaenidae (Sanderson & Wassersug,

171   1993), and given that RBINS 879a-f represents an advanced balaenid species (as judged from its

172 placement in the phylogenetic hypothesis of relationships presented in this paper), there is no

173 reason to propose a fundamentally different skull/body ratio in this specimen.

174

175 *Phylogenetic analysis*

176 A total of 153 morphological characters were coded for 42 taxa including 3 archaeocetes used as

177 outgroups. The taxonomic sampling adopted here includes representative taxa from all the known

178 mysticete radiations. The family Balaenidae was represented by 11 taxa including *Morenocetus*

179 *parvus*; Neobalaenidae was represented by *Caperea marginata* and *Miocaperea pulchra*. The

180 Pliocene *Eubalaena* sp. from Tuscany was included in a phylogenetic analysis for the first time.

181 Characters were coded based on direct examination of specimens and on the literature listed in the

182 Supplementary Information file together with both character list and taxon x character matrix.

183 Only 2 characters were coded from baleen morphology; all the other characters were coded from

184 the analysis of the skeletal anatomy of mysticetes and archaeocetes. All characters were unordered

185 and unweighted and followed the outgroup polarization criterion.

186 Character choice was made bearing in mind the goal of maximum reduction of homoplasy in the

187 dataset. This goal was achieved by examining the homoplasy level shown by each character states

188 published by Bisconti (2008, 2011), Bisconti et al. (2013), Bisconti & Bosselaers (2016), Marx

189 (2011) and Boessenecker & Fordyce (2015). Bisconti et al. (2013) and Bisconti & Bosselaers

190 (2016) published the consistency index (hereinafter abbreviated as CI) of all the synapomorphies

191 supporting named nodes. Characters with CI < 1 were considered homoplastic and were excluded

192 from the present dataset. As far as characters from other papers are concerned, it was more difficult

193 to decide whether a character had a homoplastic distribution or not. To get decisions, character

194 states were mapped on published phylogenetic hypotheses and their distributions were assessed by

195   eye; in the case a character showed scattered distribution across the branches of the Mysticeti tree,

196   then the application of Fitch's (1971) parsimony allowed to decide if the character could be

197   considered homologous or not in those branches.

198   The taxon x character matrix was treated by TNT (Goloboff et al., 2008) with default parameters

199   for New Technology Search. The synapomorphies were mapped onto the resulting cladogram and

200   were listed through the dedicate commands in TNT. Number of steps added by each character was

201   calculated at relevant nodes to determine whether the character state constituted an ambiguous or

202   unambiguous synapomorphy at the node.

203

204   *Stratigraphic consistency index and determination of divergence dates*

205   The degree of agreement between the branching pattern and the stratigraphic occurrence of the

206   taxa was assessed by the calculation of the Stratigraphic Consistency Index (hereinafter, SCI)

207   following the method described by Huelsenbeck (1994; see also discussion in Bisconti, 2007).

208   Stratigraphic ages of the taxa were obtained from the Paleobiology Database available at

209   https://paleobiodb.org and mainly compiled by Mark D. Uhen. Adjustments to the ages of the

210   specimens provided by Marx & Fordyce (2015) were also included where necessary. Stratigraphic

211   ages of the taxa are provided in the Supplementary Information file published in the website of

212   this Journal. The stratigraphic intervals of occurrence of the taxa were used to constrain the

213   divergence dates of the branches included within Balaenoidea in order to get information about

214   the origin of the living right whale and bowhead whale species.

215

216   **Systematic Paleontology**

217

218   Class MAMMALIA Linnaeus, 1758

219   Order CETACEA Brisson, 1762

220   Clade PELAGICETI Uhen, 2008

221   Clade NEOCETI Fordyce and de Muizon, 2001

222   Suborder MYSTICETI Cope, 1891

223   Infraorder CHAEOMYSTICETI Mitchell, 1989

224   Parvorder BALAENOMORPHA Geisler & Sanders, 2003

225   Superfamily BALAENOIDEA Flower, 1865

226   Family BALAENIDAE Gray, 1825

227

228   Balaenidae gen. et sp. indet.

229

230   *Material*. Cervical vertebrae complex RBINS M. 881 (IG 8444). This specimen was first figured

231   and described as the cotype of *Balaena belgica* by Abel (1941, p. 13; pl. 2, fig. 9), and later

232   commented and re-illustrated by Plisnier-Ladame & Quinet (1969, fig. 1; pl. 1 and 2, associated

233   to neurocranium RBINS M. 879).

234

235   *Locality and horizon information*. The specimen was found on March 6, 1914 by G. Hasse in the

236   docks of Antwerp harbor (northern Belgium), more precisely in the "darses I-II" (Fig. 1). Abel

237   (1941) mentions an origin in the "Scaldisien" for this specimen. Now disused, this

238   chronostratigraphic regional unit is roughly equivalent to the Lillo Formation, a latest early to

239   Late Pliocene lithostratigraphic unit (latest Zanclean to Piacenzian; Laga et al., 2006; De Schepper

240   et al., 2009; see Fig. 2).

241

242   *Description.* The specimen includes a complex formed by fused cervical vertebrae (Fig. 3).

243   Anteriorly, only the ventral portions of the articular facets of the atlas for the occipital condyles of

244   the skull are preserved. The articular surfaces of the facets are highly concave and wide

245   (measurements are provided in Table 1). The articular facets are separated dorsally by a wide

246   concavity that corresponds to the ventral border of the neural canal. Posteriorly, the articular facet

247   of the 7th cervical vertebra for the 1st thoracic vertebra is highly concave and shows a uniformly

248   convex lateral border. Laterally, the ventral apophysis of the atlas protrudes laterally and ventrally

249   and is separated from a small fragment of the ventral apophysis of the axis by a narrow,

250   dorsoventral groove that is slightly oblique in lateral view. The transverse grooves that are

251   sometimes observed in the cervical complexes of *Caperea marginata* and in balaenid species

252   (Bisconti, 2012) are not seen in this specimen. No additional characters can be described due to

253   the poor preservation of the specimen.

254   Moran et al. (2014) published a study on the ontogenetic fusion of the cervical vertebrae in the

255   extant bowhead whale *Balaena mysticetus*, observing that total fusion of the vertebral centra in the

256   cervical region occurs between 10 and 20 years after birth. In RBINS M. 881 the fusion appears

257   complete as the grooves observed at the dorsolateral and ventrolateral corners of the cervical

258   complex are not deep and do not allow to separate the centra. It is thus possible that RBINS M.

259   881 belonged to an individual of an age included between 10 and 20 years. However, this

260   hypothesis should be tested with comparisons to the fusion pattern of vertebral centra in the

261   cervical region of *Eubalaena* in a way to get a more accurate estimate of the individual age of this

262   specimen. Unfortunately, such a study is still lacking.

263

264   *Discussion and taxonomic decision.* The specimen represents a complex that presumably includes

265   all the cervical vertebrae of a balaenid whale. The morphology is consistent with that of Balaenidae

266   as in *Caperea marginata* the ventral apophysis projects much more ventrally and the outline of the

267   posterior articular surface of the 7th cervical vertebra is squared in posterior view. In other

268   mysticetes the cervical vertebrae are not fused; fusion may occasionally occur in the presence of

269   pathological processes, but the involvement of all the cervical vertebrae is extremely rare. It is

270   possible to distinguish the cervical vertebrae of the living species of *Eubalaena* from the extant

271   *Balaena mysticetus* based on: (1) shape of the neural apophysis, (2) shape of the neural canal, and

272   (3) size, shape and orientation of the ventral apophysis of the atlas. Unfortunately, the specimen

273   RBINS M. 881 is too poorly preserved to allow a safe identification; in fact, in this specimen the

274   neural apophyses are not preserved, the neural canal is only partly preserved, and the ventral

275   apophyses of the atlas are largely damaged and worn. For this reason, we assign RBINS M.881 to

276   Balaenidae gen. et sp. indet. Consequently, this decision implies that this specimen cannot be

277   designated as the holotype of the species *Eubalaena belgica*. Therefore, as Abel (1941) designated

278   RBINS M. 881 as the cotype of '*Balaena belgica* and now we assign it to gen. et sp. indet., it

279   follows that both '*Balaena belgica* and its recombination, *Eubalaena belgica*, are nomina dubia.

280

281   Balaenidae gen. et sp. indet.

282

283   *Material.* Fragment of right maxilla RBINS M. 880a-c (IG 8652), mentioned as a fragment of

284   mandible by Plisnier-Ladame & Quinet (1969, p. 2), but never figured.

285

286   *Locality and horizon information*. The specimen was found at Oorderen during the excavation of

287   the first Kruisschans lock of the Antwerp harbor at a depth of 7.80 m under the sea level (Fig. 1).

288   The specimen originates from the Lillo Formation ("Scaldisien"), in a level slightly lower than the

289   neurocranium RBINS M. 879 (see below). Its geological age falls in the range 3.7-2.8 Ma (latest

290   Zanclean-Piacenzian; De Schepper et al., 2009; Fig. 2).

291

292   *Description.* The specimen includes part of the proximal portion of the right maxilla of a balaenid

293   whale (measurements are provided in Table 1). The maxilla is transversely compressed and bears

294   an arched and thin lateral border (Fig. 4). Posteriorly, three infraorbital foramina are observed;

295   ventrally a long groove for the vasculature of the baleen-bearing tissue runs along the whole ventral

296   surface of the bone. Such a surface is lateromedially and anteroposteriorly concave. It is not clear

297   if the orientation of this fragment is more similar to *Eubalaena* and *Balaenula* (in these taxa the

298   posterior portion of the maxilla is nearly horizontal in lateral view) or to *Balaena mysticetus* (in

299   this species the posterior portion of the maxilla projects dorsally and anteriorly) or to *Balaenella*

300   *brachyrhynus* (in this species the posterior portion of the maxilla distinctly projects

301   anteroventrally).

302

303   *Discussion and taxonomic decision.* The specimen RBINS M. 880a-c represents a balaenid

304   maxilla. In fact it shows a distinctive arch in lateral view, it is transversely compressed, and it

305   displays a longitudinally-developed groove for the vasculature of the baleen-bearing tissue.

306   Unfortunately, it is impossible to reconstruct the original orientation of this fragment in the skull;

307   this, together with the lack of the anterior portion of the rostrum and of the lateral process of the

308   maxilla, prevents a safe taxonomic assignment. For this reason, we assign RBINS M. 880a-c to

309   Balaenidae gen. et sp. indet.

310

311   Genus *Eubalaena* Gray, 1864

312

313   *Type species. Eubalaena australis* Desmoulins, 1822.

314

315   *Holotype.* An unnumbered skeleton housed at the Museum National d'Histoire Naturelle, Paris,

316   France.

317

318   *Diagnosis of genus.* Balaenid cetacean characterized by all the characters diagnostic of the

319   *Eubalaena + Balaenula* clade (i.e., rostrum and supraorbital process of the frontal form a right

320   angle in lateral view, nasal and proximal rostrum horizontal in lateral view, orbitotemporal crest

321   well developed on the dorsal surface of the supraorbital process of the frontal, and zygomatic

322   process of the squamosal directed anteriorly so that the posterior wall of the temporal fossa cannot

323   be observed in lateral view) and by the following, exclusively *Eubalaena* characters: vertically-

324   oriented squamosal, protruding lambdoid and temporal crests, convex and protruding

325   supramastoid crest, dome-bearing supraoccipital, wide and rounded anterior process of

326   supraoccipital, and pars cochlearis of petrosal protruded cranially.

327

328   *Discussion.* Bisconti (2003) provided the last diagnosis of *Eubalaena* published up to the present

329   work; diagnostic characters included: gigantic body size (maximum body length approaching 22

330   m), rostrum and supraorbital process of frontal form a right angle, nasal and proximal rostrum

331 horizontal, ascending temporal crest well developed on the dorsal surface of the supraorbital

332 process of the frontal, vertically-developed squamosal, zygomatic process of the squamosal

333 directed anteriorly so that the posterior wall of the temporal fossa cannot be observed in lateral

334 view, protruding lambdoidal and temporal crests, convex and protruding lateral squamosal crest,

335 exoccipital squared in lateral view, dome-bearing supraoccipital shield with sagittal crests, wide

336 anterior process of supraoccipital, pars cochlearis cranially-protruding, and superior process of

337 petrosal cranially-protruding. Bisconti's (2003) diagnosis is certainly useful to separate extant

338 *Eubalaena* from other living balaenids but it may be of limited help when trying to separate fossil

339 *Eubalaena* species from other living and fossil balaenids. In particular, the above diagnosis

340 includes characters that are shared with the extinct *Balaenula* lineage: rostrum and supraorbital

341 process form a right angle, nasal and proximal rostrum horizontal, ascending temporal crest

342 (orbitotemporal crest *sensu* Mead & Fordyce, 2009) well developed on the dorsal surface of the

343 supraorbital process of the frontal, and exoccipital squared in lateral view. All these characters can

344 be observed also in *Balaenula astensis* or in *Balaenula balaenopsis*. A more detailed diagnosis of

345 *Eubalaena* allowing to separate this genus from all the other living and extinct balaenid taxa

346 includes the characters listed in the Emended diagnosis of genus provided above.

347

348 *Eubalaena* sp. indet.

349

350 *Material.* Left humerus RBINS M. 2280, mentioned by Plisnier-Ladame & Quinet (1969, p. 2),

351 but never figured.

352

353   *Locality and horizon information*. Antwerp area. There is no precise locality data available for this

354   specimen. A stratigraphic assessment is currently impossible.

355

356   *Description.* This well-preserved, robust left humerus shows a highly rounded proximal articular

357   head that is anteriorly bounded by a protruding deltoid tuberosity; the latter is triangular in lateral

358   view (measurements are provided in Table 1). The diaphysis shows straight anterior and posterior

359   borders (Fig. 5); the posterior border is shorter than the anterior border, as it terminates more

360   proximally due to the development of the articular facet for the olecranon process of the ulna. Such

361   a facet protrudes posteriorly and occupies part of the posterior border of the humerus. The

362   anteroventral corner of the humerus protrudes anteriorly forming a kind of triangular tuberculum.

363   The articular facets for radius and ulna are separated by a transverse protrusion that is triangular

364   in lateral view.

365

366   *Discussion and taxonomic decision.* The morphology of the articular head of the humerus RBINS

367   M. 2280 is consistent with both *Eubalaena* and *Balaena*. In *Eubalaena glacialis* the external

368   border of the lateral surface of the articular head shows a posterior concavity that is not seen in

369   *Balaena mysticetus* (Benke, 1993). Unfortunately, RBINS M. 2280 is worn in that region thus

370   preventing a clear understanding of its morphology. More distally, the articular facet for the

371   olecranon is well developed as seen in the extant *Eubalaena* species while in *Balaena mysticetus*

372   it is largely reduced. Benke (1993) showed that the posterior border of the diaphysis in *Balaena*

373   *mysticetus* is uniformly concave and short and that the deltoid tuberosity is less protruding than in

374   *Eubalaena glacialis*. In the latter, the posterior border of the diaphysis is more elongated

375   (resembling that of RBINS M. 2280) and the deltoid tuberosity is triangular and protruding. In the

376 humerus RBINS M.2280 the deltoid tuberosity is triangular and protruding as in *E. glacialis*.

377 However, the posterior border of the diaphysis of RBINS M. 2280 is straighter than that observed

378 in *E. glacialis*.

379 Comparative analysis shows, thus, that the humerus RBINS M. 2280 is closer to *Eubalaena* than

380 to *Balaena*, as it shares with *E. glacialis* the presence of (1) well-developed and protruding

381 articular facet for the olecranon process, (2) triangular and protruding deltoid tuberosity and, (3)

382 comparatively long posterior border of the diaphysis. These shared characters allow inclusion of

383 RBINS M. 2280 within *Eubalaena*. However, the different shape of the posterior border of the

384 diaphysis and the lack of information about the shape of the lateral outline of the articular head do

385 not allow inclusion of this specimen within *E. glacialis* or other extant *Eubalaena* species. RBINS

386 M. 2280 is thus assigned to *Eubalaena* sp. indet.

387 When compared to the extant *Eubalaena* species, this humerus is particularly long suggesting that

388 it belonged to a large individual. The total proximodistal length of RBINS M. 2280 is 683 mm,

389 which is greater than the maximum humeral lengths published by Benke (1993) for *Balaena*

390 *mysticetus* (i.e., 605 mm), *Eubalaena glacialis* (555 mm), and *E. australis* (619 mm), and by

391 Omura (1958) for *E. japonica* (556 mm). Based on this comparison, we suggest that the humerus

392 RBINS M. 2280 belonged to an individual that was longer than 16.5 m. This is the first report of

393 a gigantic right whale in the fossil record of the North Sea.

394

395 *Eubalaena ianitrix* sp. nov. LSID: urn:lsid:zoobank.org:act:F17C4DCA-FF1B-4EA4-9E6B-

396 6C1EED448745

397

398   *Derivation of name.* The specific name *ianitrix* derives from Ianus, the Roman God who was the

399   guardian of passages, gates and doors. This name is related to the discovery of the holotype in the

400   locks (or entrances) of the Antwerp harbor.

401

402   *Holotype.* The holotype is housed at the Royal Belgian Institute of Natural Sciences, Brussels,

403   Belgium, and bears the inventory number M. 879a-f, Reg. 4019, I.G. 8652 (all the numbers refer

404   to the same individual). It includes a partial skull (M. 879a), right squamosal and exoccipital (M.

405   879b), left squamosal and exoccipital (M. 879c), fragment of a maxilla (M. 879d), fragment of the

406   right supraorbital process of the frontal (M. 879e), fragment of the left supraorbital process of the

407   frontal (M. 879f). It was first figured and described as *Balaena belgica* by Plisnier-Ladame &

408   Quinet (1969, p. 2; pl. 1-2, associated to cervical complex RBINS M. 881).

409

410   *Type locality.* The neurocranium RBINS M. 879a-f was discovered in Oorderen (Fig. 1) during

411   the excavation of the first Kruisschans lock (*'première écluse du Kruisschans'*, now named Van

412   Cauwelaertsluis) of the Antwerp harbor (Plisnier-Ladame & Quinet, 1969). Geographic

413   coordinates: 51°16'32"N- 04°19'51"E. As mentioned above, the maxilla RBINS M. 880a-c was

414   found at the same site. However, based on labels associated to specimens, the neurocranium was

415   found at a depth of 3.70 m under the sea level, whereas the maxilla was found at a depth of 7.80

416   m under the sea level, therefore most likely not representing the same individual.

417

418   *Type horizon.* Based on data associated to the neurocranium RBINS M. 879a-f, Misonne (1958)

419   indicated an origin in the Kruisschans Sands (*'Sables du Kruisschans'*; Fig. 2) in the *'zone à*

420   *Cardium'*, and a Merksemian ('Merxemien') stage, a stage assignation later confirmed by Plisnier-

421 Ladame & Quinet (1969). Now disused, this regional stage was first introduced by Heinzelin

422 (1955a), including the Kruisschans Sands and Merksem Sands, together with an underlying gravel

423 layer (Laga & Louwye, 2006). Both the Kruisschans Sands Member and Merksem Sands Member

424 are now part of the Lillo Formation, constituting its two youngest members (Vandenberghe et al.,

425 1998; Laga et al., 2006).

426 In published sections of the Pliocene and Quaternary layers at the Kruisschans locks (including

427 sections in a new lock parallel to the ancient lock, 'Ecluse Baudouin'), a clayey sand layer

428 containing a high concentration of shells of the bivalve *Laevicardium* (first named *Cardium*)

429 *parkinsoni* and isolated cetacean bone fragments is reported at a depth of 5.5-7 m (Heinzelin, 1952,

430 1955b). This shell layer is located about 1 m above the base of the Kruisschans Sands. It is

431 therefore tempting to propose that the 'zone à *Cardium*' mentioned by Misonne (1958) for the

432 horizon of the skull RBINS M. 879a-f corresponds to this part of the Kruisschans Sands.

433 Dinoflagellate cysts from a section 4 km north to the Kruisschans locks give a Piacenzian (Late

434 Pliocene) age to both the Kruisschans Sands Member and the overlying Merksem Sands Member,

435 older than 2.6 Ma (as confirmed by pollens) and most likely somewhat younger than 3.7 Ma (age

436 of the base of the Lillo Formation), whereas sequence stratigraphy narrows even more their

437 temporal range to 3.2 to 2.8 Ma (De Schepper et al., 2009). RBINS M. 879a-f is therefore proposed

438 to date from that Piacenzian interval.

439 The record of fossil marine mammals in the Kruisschans Sands Member is relatively poor; only

440 the odobenid *Alachtherium antwerpiensis* and the stem phocoenid *Septemtriocetus bosselaersi* are

441 known to originate from that unit (Hasse, 1909; Lambert, 2008).

442

443 *Diagnosis. Eubalaena ianitrix* differs from *E. shinshuensis* in showing a distinctive anteroventral

444 corner in the parietal-frontal suture and in having an anterodorsally protruded squamosal-parietal

445 suture; it differs from the *Eubalaena* sp. from the early Late Pliocene of Tuscany (included in our

446 diagnosis considering that in our phylogenetic analysis it represents a true right whale species

447 needing a new species name) in having an anteriodorsally protruded squamosal-parietal suture; it

448 differs from *E. japonica* in having the pterygoid exposed in the temporal fossa, in having

449 posteromedially directed anterior borders of the palatine and in having anteriorly directed posterior

450 borders of the palatine; it differs from *E. australis* in having a less protruding anteroventral corner

451 in the parietal-frontal suture, in having an anterodorsally protruded squamosal-parietal suture, in

452 having the pterygoid exposed in the temporal fossa and in having anteriorly directed posterior

453 border of the palatine; it differs from *E. glacialis* in having a crest located at the squamosal-

454 parietal-supraoccipital suture and in having anteriorly directed posterior border of the palatine.

455 *Eubalaena ianitrix* does not possess any autapomorphy and may be distinguished from other

456 *Eubaena* species by the following combination of characters: bilateral bulge on supraoccipital with

457 presence of sagittal crest, alisphenoid exposed in the temporal fossa, and alisphenoid dorsally

458 bordered by a squamosal projection that prevents it to make contact with parietal.

459

460 **Comparative anatomy of the skull of *Eubalaena ianitrix***

461

462 The holotype specimen consists of a moderately well preserved partial skull. The skull is massive

463 and heavy and lacks part of the supraoccipital borders due to post-mortem erosion. It is subdivided

464 into six fragments that can be put together due to clear break surfaces. Measurements are provided

465 in Table 2.

466

467 *Rostrum.* Only a fragment of the right maxilla is preserved showing the typical transverse

468 compression present in Balaenidae.

469

470 *Frontal.* Due to the erosion of the anterior-most border of the supraoccipital, it is possible to

471 observe a tiny portion of the interorbital region of the frontal in dorsal view (Figs 6). Prior to the

472 erosion of the supraoccipital, that portion was superimposed by the anterior portion of the

473 supraoccipital and was not visible. Judging from what is preserved, the interorbital region of the

474 frontal was less bent than the supraoccipital suggesting that, in lateral view, the posterior portion

475 of the rostrum was nearly flat as seen in *Eubalaena glacialis*. The transverse diameter of the

476 interorbital region (measured along the inferred position of the nasofrontal suture) is *c.* 240 mm.

477 The supraorbital processes of the frontal are detached from the skull probably because post-

478 mortem damage. The supraorbital process of the frontal is anteroposteriorly narrow and bears an

479 evident but rounded orbitotemporal crest developed from the postorbital process to its

480 anteromedial border (Figs 6, 7 and 8). The orbitotemporal crest is sharper proximally and becomes

481 lower approaching the orbital rim. The right supraorbital process of the frontal is 650 mm in length

482 up to the center of the orbit. The left supraorbital process of the frontal is 712 mm in length. A

483 long groove for articulation with the maxilla is located at the anteromedial corner of the left

484 supraorbital process of the frontal (Fig. 9).

485 The optic canal is deep proximally (depth is *c.* 45 mm) and shallow distally (depth is *c.* 35 mm).

486 Proximally, the right optic canal is bordered by anterior and posterior crests whose distance is 50

487 mm proximally and *c.* 100 mm distally (Fig. 10). The anteroposterior diameter of the left optic

488   canal is 30 mm proximally at a distance of 400 mm from the orbital rim and 70 mm a few mm

489   from the orbital rim.

490   Approaching the orbit, the dorsal surface of the supraorbital process of the frontal flattens. The

491   right orbit is 170 mm in length (from the center of the postorbital process of the frontal to the

492   center of the antorbital process of the frontal) and 51 mm in height (measured from the center of

493   the orbital rim to an imaginary line joining antorbital and postorbital processes of the frontal). On

494   the right side, antorbital and postorbital processes are similar in size but on the left side, the

495   postorbital process is more robust than the antorbital process (Figs 7 and 8). The longitudinal axis

496   of the supraorbital process of the frontal is perpendicular to the imaginary line joining antorbital

497   and postorbital processes. This suggests that, in the living animal, the supraorbital process of the

498   frontal formed an approximately right angle with the lateral process of the maxilla and, thus,

499   resembling the condition observed in the right whale of the genus *Eubalaena* and the fossil

500   *Balaenula*.

501   The frontal of *Eubalaena ianitrix* shares the following characters with the living *Eubalaena* and

502   *Balaenula*: presence of an evident orbitotemporal crest developed from the postorbital process to

503   the anteromedial corner of the supraorbital process of the frontal, lack of dorsoventral compression

504   along most of the length of the supraorbital process of the frontal (as seen in *Morenocetus parvus*,

505   *Balaena mysticetus* and *Balaenella brachyrhynus*), presence of a right angle between supraorbital

506   process of the frontal and the lateral process of the maxilla in lateral view, interorbital region of

507   the frontal clearly angled with respect to the dorsoventral inclination of the supraoccipital. The

508   articular groove for the maxilla combined with the short anteroposterior diameter of the proximal

509   portion of the supraorbital process suggests that the ascending process of the maxilla was short

510   and wide like that typically observed in the other Balaenoidea where this structure has been

511   described (Bisconti, 2012 and literature therein). The short exposure of the interorbital region of

512   the frontal on the dorsal surface of the skull and the exclusion of the parietal from exposure at

513   cranial vertex are typical characters of living and fossil Balaenoidea.

514

515   *Parietal.* The parietal is evident on the lateral sides of the skull and at the cranial vertex due to the

516   erosion of the anterior-most border of the supraoccipital (Fig. 6). Originally, the parietal was

517   covered by the anterior border of the supraoccipital forming the nuchal crest. The frontal border

518   of the parietal is superimposed on the interorbital region of the frontal obliterating it in dorsal view.

519   More laterally, the frontal border descends ventrally and posteriorly and borders the posterodorsal

520   portion of the supraorbital process of the frontal and forming an anteriorly convex coronal suture.

521   Posteriorly to the supraorbital process of the frontal, the coronal suture forms a curve with anterior

522   concavity and projects ventrally and posteriorly (Figs 7, 8).

523   The shape of the coronal suture is different in different balaenoid lineages. In the skull of *Caperea*

524   *marginata* as seen in lateral view, the frontal border of the parietal gently descends from an

525   anterodorsal point to a point located posterventrally in a straight-to-slightly convex line located

526   dorsally to the supraorbital process of the frontal. This shape of the frontal border of the parietal

527   is shared also with *Balaena mysticetes*, *B. montalionis*, *B. ricei* and *Balaenella brachyrhynus*. In

528   the fossil *Miocaperea pulchra*, the right parietal shows a slightly different condition; in this species

529   a distinctive anteroventral corner is located along the frontal border of the parietal (Bisconti, 2012).

530   The anteroventral corner is present also in the species belonging to *Balaenula* and *Eubalaena* and

531   in *Eubalaena ianitrix* (Figs 7, 8). In *Eubalaena australis*, posterior to the anteroventral corner, the

532   frontal border shows a strong ventral concavity and a rounded shape making it distinct from the

533   parietal of all the other balaenoid species.

534 The supraoccipital border of the parietal protrudes laterally and, together with the lateral border of

535 the supraoccipital, forms the temporal crest. The temporal crest protrudes laterally and forms a sort

536 of short roof of the temporal fossa in such a way that it prevents the medial wall of the temporal

537 fossa (formed by the external surface of the parietal) from being observed in dorsal view. The

538 external surface of the parietal is widely concave. Along the anteroposterior axis of the skull, the

539 parietal appears short and high. The dorsal portion of the squamous border is anteroposteriorly

540 elongated and bears a weak crest; the ventral portion of the squamous border forms a highly

541 interdigitated suture with the squamosal and projects ventrally.

542 Among Balaenidae, a crest along the squamous border has been detected as a synapomorphy of

543 *Balaena* and *Balaenella* by Bisconti (2005a) and Churchill et al. (2012) as it is absent from

544 *Balaenula* and *Eubalaena*. It is not clear whether this crest is present in *Morenocetus* and

545 *Peripolocetus*. The shape of the frontal border of the parietal differs from that observed in *Balaena*

546 and *Balaenella* as it shows an undulating development; in *Balaena* and *Balaenella* the frontal

547 border of the parietal proceeds posteroventrally as a straight line. A highly interdigitated ventral

548 portion of the squamous border of the parietal is also observed in a subadult individual of *E.*

549 *australis* (specimen NBC RGM 24757).

550 The squamous border of the parietal has distinctive characters in different balaenoid lineages. In

551 *Caperea marginata*, the dorsal portion of the squamous border projects posteriorly to meet the

552 supraoccipital (Bisconti, 2012). This character is also observed in *Balaena mysticetus* adult NBC

553 RGM 373 and foetal NBC RGM 31116; the character was also illustrated by Cuvier, 1823; see

554 Bisconti, 2003 for an image), *Eubalaena australis* adult IZIKO 2284, subadult NBC RGM 24757

555 and foetal IZIKO ZM 38950) and in the Pliocene *Eubalaena* sp. from Tuscany (Bisconti, 2002).

556 In *Miocaperea pulchra* and *Balaenella brachyrhynus* the dorsal portion of the squamous border is

557   nearly vertical. In *Eubalaena glacialis*, *E. japonica*, *Balaenula astensis* and *Eubalaena ianitrix* the

558   dorsal portion of the squamous border projects anteriorly forming a finger-like structure that is

559   deeply wedged between the parietal and the supraoccipital.

560

561   *Supraoccipital.* The supraoccipital is strongly built and represents the largest bone of this skull

562   (Fig. 6). Parts of the anterior and lateral borders are missing due to post-mortem erosion of the

563   skull and to damage done during the collection and preparation of the skull. The supraoccipital is

564   wide and, as preserved, shows a convex lateral border and a widely rounded anterior border. The

565   anteroposterior length (from the anterior border to the inferred position of the dorsal edge of the

566   foramen magnum) is *c.* 531 mm; the transverse diameter is *c.* 350 mm anteriorly and *c.* 590 mm

567   at mid-length. The external occipital protuberance, located on the anterior surface of the

568   supraoccipital, is dorsally convex and forms a wide dome bordered by bilateral fossae located near

569   the lateral borders of the supraoccipital. The dome consists of relief posteriorly subdivided by the

570   interposition of a triangular, parasagittal fossa. There is a low sagittal crest located posteriorly to

571   the dome. In lateral view, the dome is clearly visible as it protrudes dorsally and is not obliterated

572   to view by the temporal crests. Before the post-mortem erosion of the skull, the supraoccipital

573   formed a dorsal roof to the temporal fossa preventing the parietal from being observed in dorsal

574   view.

575   In the genus *Eubalaena*, the supraoccipital is anteriorly wide and rounded and displays an external

576   occipital protuberance that is dome-shaped. These characteristics of the supraoccipital are

577   observed in all the living *Eubalaena* species, in the fossil *E. shinshuensis* and in the *Eubalaena* sp.

578   described by Bisconti (2002) from the Pliocene of Tuscany. Subtle differences in the characters of

579   the dome could be used for differentiating the species of *Eubalaena* but it is not completely clear

580   whether the differences are due to individual variation or have taxonomic value. Bisconti (2002)

581   described a sagittal crest on the external occipital protuberance and a series of five parasagittal

582   crests posterior to it in a Pliocene *Eubalaena* sp. The five parasagittal crests are not observed in

583   other *Eubalaena* species. A single sagittal crest is present in *Eubalaena australis* (NBC RGM

584   24757), *Eubalaena glacialis* (AMNH 42752, MSNT 264) *E. japonica* (Omura, 1958) and

585   *Eubalaena ianitrix*.

586   The external supraoccipital protuberance is formed by a bilateral bulge in *Eubalaena australis*

587   (NBC 24757), *E. glacialis* (AMNH 42752), *Eubalaena* sp. (Bisconti, 2002), and *E. ianitrix*, and

588   by a single axial bulge in *E. japonica* and *E. shinshuensis* (Kimura, 2009). The external

589   supraoccipital protuberance is a single bulge also in *Balaena mysticetus*, *Balaena montalionis*,

590   *Balaena ricei* and *Balaenella brachyrhynus* but in these species the anterior portion of the

591   supraoccipital is transversely constricted while in the species belonging to *Morenocetus*,

592   *Balaenula* and *Eubalaena* the anterior portion of the supraoccipital is transversely wide.

593   Observations on skulls belonging to living species suggest that the lateral borders of the

594   supraoccipital potentially undergo morphological change during ontogeny. In *Eubalaena*

595   *australis*, the lateral border of the supraoccipital is externally convex in fetal and subadult

596   individuals (ISAM ZM 38950, NBC RGM 24757). Omura (1958) observed that in adult

597   individuals of *Eubalaena glacialis* the lateral border of the supraoccipital is more concave that in

598   *E. japonica*. However, in the images provided by True (1904), an adult individual of *Eubalaena*

599   *glacialis* has a continuously convex lateral border of the supraoccipital. It is possible that Omura's

600   (1958) observation was related to differences in the point of view from which the skulls were

601   observed (Yamada et al. 2006).

602

603   *Vertex*. Based on Mead & Fordyce (2009, and literature therein) terminology, the vertex is the

604   highest portion of the skull. In mysticetes it is formed by a mosaic of bones including

605   supraoccipital, parietal, frontal and some posteromedial elements of the rostrum nasal and the

606   ascending process of the premaxilla and of the maxilla). In *E. ianitrix*, the supraoccipital overlaps

607   onto the parietal and prevents it from being observed in dorsal view (Fig. 6). The parietal is

608   superimposed onto the interorbital region of the frontal that is, thus, scarcely visible in dorsal view.

609   The only portion of the interorbital region of the frontal that can be observed is that that is

610   immediately posterior to the nasofrontal suture. Judging from the articular groove present on the

611   anteromedial surface of the supraorbital process of the frontal, the ascending process of the maxilla

612   had a limited posterior extension resembling other living and fossil Balaenoidea.

613   The supraoccipital superimposition on the parietal and the parietal superimposition on the

614   interorbital region of the frontal are synapomorphies of Balaenidae and Neobalaenidae and are not

615   shared with other mysticete taxa (Bisconti, 2012 and literature therein). The lack of parietal

616   exposure at the cranial vertex is another exclusive feature of Balaenidae and Neobalaenidae and is

617   observed in all the living and fossil taxa belonging to these groups (Churchill et al., 2012; Bisconti,

618   2003).

619

620   *Exoccipital.* The lateral portion of the exoccipital is a wide and flat surface with external border

621   squared (Fig. 11). Only the left paroccipital process is preserved and appears strong and rugose in

622   ventral view. A squared external border of the exoccipital is observed in *Eubalaena japonica* and,

623   at a lesser extent, in *Eubalaena australis*. In *E. glacialis* the external border has a rounder shape

624   than in those species. In *Balaena mysticetus* and *B. montalionis* the external border of the

625   exoccipital appears anterolaterally round with a distinctive lateroventral corner that is observed

626 also in *E. glacialis* but that seems absent in *E. japonica* (Omura, 1958). In lateral view, the

627 exoccipital has a squared shape in *E. glacialis*, *E. australis*, *E. japonica* and the species belonging

628 to *Balaenula* but it is not clear whether a squared shape is also present in *Eubalaena ianitrix*.

629 The occipital condyle is wide, reniform and its surface for articulation with the atlas is nearly flat

630 along both the dorsoventral and the lateromedial axes. The main axis of the occipital condyle is

631 oriented from a posteroventral point to an anterolateral point. There is a wide intercondyloid fossa

632 located ventrally between the condyles. The condyles are not in contact each other ventrally or

633 dorsally. The maximum anteroposterior diameter of the occipital condyle is 190 on the right side

634 and 170 on the left side; the maximum lateromedial diameter of the occipital condyle is 101 on the

635 right side and 107 on the right side. The condyles surround a wide foramen magnum whose dorsal

636 border is not preserved. The maximum tansverse diameter of the foramen magnum is 145 mm and

637 its dorsoventral diameter is inferred to be *c.* 140 mm based on a nearly circular outline with a slight

638 dorsoventral compression as seen in other balaenid species. The distance between the external

639 borders of the occipital condyles is *c.* 350 mm.

640

641 *Squamosal*. Right and left squamosals are partly broken; breakage lines are straight enough to

642 allow an easy reconstruction of this part of the skull by putting the broken portions of the

643 squamosals in place through right connections (Figs 7, 8).

644 The parietal margin of the squamosal forms the squamosal-parietal suture. Dorsally, this suture

645 projects anteriorly making it possible for the squamosal to be deeply inserted between the

646 supraoccipital and the parietal. More ventrally, the squamosal-parietal suture is highly

647 interdigitated.

648 The squamosal plate is dorsoventrally and anteroposteriorly concave and, in lateral view, it is

649 hidden by the anterior and ventral development of an anteriorly convex supramastoid crest. The

650 supramastoid crest is protruding anterolaterally and shows a widely rounded anterior shape. The

651 supramastoid crest is separated from the zygomatic process of the squamosal by a wide anterior

652 concavity. The zygomatic process of the squamosal is short and stocky; its main axis projects

653 laterally and ventrally in dorsal view.

654 The squamosal has a clear dorsoventral development as typically observed in Balaenidae. Its

655 dorsoventral diameter is 550 mm on the external surface (from the exoccipital-squamosal suture

656 to the anterior end of the zygomatic process of the squamosal) of the right squamosal. The glenoid

657 fossa of the squamosal is largely eroded; what remains suggests that it was flat or scarcely concave

658 as seen in other typical balaenid whales. The glenoid fossa of the right squamosal is 470 mm in

659 anteroposterior length.

660 Posterodorsally, the site for the articulation with the posterior process of the petrotympanic is

661 developed ventrally to the exoccipital-squamosal suture and is ventrally bordered by a crest that

662 separates it from the external acoustic meatus. Both this site and the external acoustic meatus are

663 represented by transverse and tube-like concavities developed along the dorsal and posterior

664 portion of the squamosal. The posterior border of the foramen ovale is made of the squamosal and

665 the pterygoid.

666 The squamosal of *Eubalaena ianitrix* shows the following typical balaenid characters: dorsoventral

667 elongation, reduction of the zygomatic process of the squamosal, scarcely concave glenoid fossa

668 of the squamosal, widely rounded supramastoid crest in lateral view. In *Balaenella* and in the

669 species of *Balaena* the squamosal is also posteroventrally oriented (Bisconti, 2000) but this

670 character is not observed in *E. ianitrix*. Rather, the squamosal of *E. ianitrix* appears more vertical

671   resembling *Morenocetus*, *Balaenula* and the living species of *Eubalaena*. In *Balaenella*

672   *brachyrhynus*, *Balaena mysticetus*, *B. ricei*, and *B. montalionis* the zygomatic process of the

673   squamosal projects more laterally allowing the view of the posterior wall of the temporal fossa

674   formed by the squamosal plate. In *Eubalaena*, *Balaenula* and *E. ianitrix* this is not the case as the

675   zygomatic process of the squamosal projects anteriorly and prevents the posterior wall of the

676   temporal fossa from being observed in lateral view.

677

678   *Alisphenoid.* The alisphenoid is exposed in the temporal fossa. It has a triangular shape. It is

679   bordered anteriorly by the supraorbital process of the maxilla, ventrally by the palatine, and

680   dorsally and posteriorly by the squamosal.

681   The alisphenoid is exposed in the temporal fossa in *Eubalaena glacialis* and *E. japonica* but it is

682   not clear whether such an exposure occurs also in *E. australis*. In fetal specimen (IZIKO ZM

683   38950) the alisphenoid is observed in the temporal fossa but in subadult individual (NBC RGM

684   24757) the alisphenoid is only visible in ventral view and does not appear in the temporal fossa as

685   the ventral border of the squamosal superimposes onto it. In *Balaena mysticetus*, *B. brachyrhynus*,

686   and in the genus *Balaenula* the alisphenoid is inferred to be exposed in the temporal fossa based

687   on the articular pattern of squamosal and parietal. The alisphenoid was originally bordered by the

688   squamosal dorsally and posteriorly and by the parietal dorsally and anteriorly, by the palatine

689   ventrally.

690

691   *Temporal fossa.* The temporal fossa of *E. ianitrix* is dorsally overhung by the lateral projection of

692   the temporal crest formed by the lateral border of the supraoccipital and the dorsal border of the

693   parietal (Fig. 6). The lateral extension of the temporal crest is difficult to assess because the lateral

694   edge of the supraoccipital and the dorsal border of the parietal are damaged. The medial wall of

695   the temporal fossa is formed by parietal, squamosal and alisphenoid. The alisphenoid is not in

696   contact with the parietal; the parietal-squamosal suture is highly interdigitated ventrally but,

697   dorsally, the squamosal forms a digit-like anterior protrusion that is deeply inserted between the

698   supraoccipital and the parietal. The medial wall of the temporal fossa is concave both

699   dorsoventrally and anteroposteriorly. The posterior wall of the temporal fossa is formed by the

700   squamosal and shows an anterior concavity. Lateral to the posterior wall of the temporal fossa, the

701   supramastoid crest protrudes anteriorly and forms the lateral border of the squamosal fossa.

702   The general features of the temporal fossa of *E. ianitrix* are also observed in *Eubalaena glacialis*

703   and *E. japonica*. *Eubalaena australis* differs in the lack of exposure of the alisphenoid in the

704   temporal fossa at adulthood. In the Pliocene *Eubalaena* sp. from Tuscany (Bisconti, 2002) and

705   *Eubalaena shinshuensis* (Kimura, 2009) the digit-like projection of the anterodorsal portion of the

706   squamosal is absent. In *Balaenula* the posterior apex of the lambdoid crest is located much more

707   anteriorly than in any species belonging to *Eubalaena*, *Balaena* and *Balaenella* and this makes its

708   temporal fossa anteroposteriorly smaller; moreover, in *Balaenula astensis* the posterior wall of the

709   temporal fossa is mainly flat along the dorsoventral axis (Bisconti, 2000, 2003).

710

711   *Palatine.* The palatine is almost rectangular in ventral view (Fig. 10). It is an elongated bone that

712   is anteriorly in contact with the maxilla and posteriorly with the pterygoid. As typically observed

713   in Balaenidae, the palatine is ventrally superimposed on the ventral lamina of the pterygoid that

714   appears, in ventral view, as a small stripe of bone close to the posterior limit of the skull. The

715   ventral surface of the palatine is almost flat. The longitudinal axis of the palatine diverges from

716   the anteroposterior axis of the skull posteriorly as the posterior ends of the palatines are not in

717   contact posteriorly. The lateral lamina of the palatine ascends and contacts the squamosal, the

718   alisphenoid and the frontal.

719   The relationships of the palatine observed in *E. ianitrix* are not different from those that can be

720   observed or inferred in other living and fossil Balaenidae for which information about this bone is

721   available.

722

723   *Pterygoid.* Following Churchill *et al.* (2012), Bisconti (2000, 2005a) and Fraser & Purves (1960),

724   in Balaenidae the pterygoid appears as a small stripe of bone in ventral view. This stripe of bone

725   represents the lateral lamina of the pterygoid that is transversely elongated and approaches the

726   posterior-most border of the skull in lateral view. The pterygoid is dorsally, anteriorly and

727   posteriorly bordered by the squamosal and anteroventrally by the palatine. The posterior border of

728   the pterygoid and the anterior border of the falciform process of the squamosal contribute to delimit

729   the shape of the foramen ovale (Fig. 10).

730   Apart from *Caperea marginata*, in which the foramen ovale is within the pterygoid, the foramen

731   ovale of other balaenoids is located between the squamosal and the pterygoid. In the living species

732   the foramen ovale extends into a tube formed almost entirely by the squamosal (= infundibulum

733   of Fraser and Purves, 1960). This condition is not observed in *E. ianitrix* where the foramen ovale

734   has an elliptical shape.

735

736   **Body size estimate**

737

738   Two of the chosen methods converge towards a total body length or *c.*6-8 m. The application of

739   equation (1) based on a bizygomatic width of 1660 mm (Table 2) retrieved a total body length of

740   *c.* 13 m; this result is to be corrected by reducing it of 37-to-47%. After the correction, the resulting

741   values are respectively *c.* 8 m and *c.* 7 m.

742   The application of the regression equation (4) based on a supraoccipital length of 560 mm (Table

743   2) found a condylobasal length of *c.* 1.6 m. After having tripled and quadrupled this length, the

744   total body length was estimated between 4.74 and 6.37 m.

745   The application of the equation (2) based on an occipital breadth of 353 mm retrieved a body mass

746   of *c.* 33 t. This value is consistent with weight values obtained by Omura et al. (1958) for the North

747   Pacific right whale (*E. japonica*). We used this body mass estimate in the equation (3) and found

748   a total body length of *c.* 11 m, which is closer to the result obtained from the equation (1) before

749   the correction. It is not clear whether the results of the equation (3) need to be corrected but,

750   following the suggestions of Pyenson & Sponberg (2011), we hypothesize that a correction would

751   be necessary that should be around 40%. If we apply such a correction to the value obtained by

752   the equation (3), we find a total body length of *c.* 6.6 m that is very close to the higher results of

753   the equations (1) and (4). If we accept a total body length between 6 and 7 m then we need to apply

754   a roughly similar correction to the estimated body weight. If we reduce the estimated body weight

755   of 40% then we obtain an estimated body weight of 19.8 t.

756   We therefore estimate the total body length of the holotype specimen of *Eubalaena ianitrix*

757   between 5 and 7 m, with a body mass of *c.* 20 t.

758

759   **Phylogeny**

760

761   *Overview*

762   The phylogenetic analysis resulted in the single most parsimonious cladogram shown in Fig. 12 .

763   Tree statistics are provided in the corresponding caption. Our results confirm the monophyly of

764   Mysticeti, Chaeomysticeti and Balaenomorpha. The sister-group of Balaenomorpha is the

765   monophyletic Eomysticetidae (here represented by *Eomysticetus whitmorei*, *Tokaraia kauaeroa*

766   and *Yamatocetus canaliculatus*). Balaenomorpha is then subdivided into two sister-groups:

767   Balaenoidea and Thalassotherii (including Balaenopteridae, Eschrichtiidae, Cetotheriidae and

768   basal thalassotherian taxa including *Cophocetus*, *Aglaocetus*, *Parietobalaena*, *Isanacetus*,

769   *Uranocetus*, *Pelocetus* and *Diorocetus*). As such, the present results confirm the monophyly of

770   Balaenopteroidea (including Balaenopteridae and Eschrichtiidae) and Cetotheriidae (here

771   including *Mixocetus*, *Herentalia*, *Piscobalaena*, *Herpetocetus* and *Tranatocetus*). *Tranatocetus*

772   *argillarius* is nested here among Cetotheriidae. Although this may be due to our limited sample of

773   Cetotheriidae and related taxa, we are unable to support the monophyly of Tranatocetidae (as

774   proposed by Gol'din & Steeman, 2015), considering that *T. argillarius* (the only nominal

775   Tranatocetidae taxon included in our analysis) falls within Cetotheriidae.

776   Most surprising are the position of *Morenocetus parvus* (that will be discussed in the next

777   paragraph) and the sister-group relationships within Thalassotherii. Among Thalassotherii, four

778   monophyletic groups of family-level rank are recognized: Balaenopteridae, Eschrichtiidae,

779   Cetotheriidae and a clade including what Bisconti et al. (2013) called basal thalassotherian taxa.

780   Eschrichtiidae is the sister-group of Balaenopteridae and both form the monophyletic

781   Balaenopteroidea. Balaenopteroidea is the sister-group of a large clade including *Titanocetus*

782   *sammarinensis*, Cetotheriidae and basal thalassotherian taxa. *Ti. sammarinensis* is, in its turn, the

783   sister-group of Cetotheriidae and basal thalassotherian taxa.

784

785 *Relationships of Balaenoidea and morphological supports to nodes*

786 Our results support the monophyly of Balaenoidea with a noticeable difference with respect to

787 previously published literature (Cabrera, 1926; Bisconti, 2005; Churchill et al., 2012):

788 *Morenocetus parvus* falls outside Balaenidae + Neobalaenidae and represents the sister-group of

789 both families.

790 Nine synapomorphies support the monophyly of Balaenoidea. Three of them depends on the

791 structure of the skull: characters 37 (short exposure of interorbital region of the frontal because of

792 superimposition by the parietal), 54 (massive elongation of supraoccipital), and 55 (supraoccipital

793 is superimposed onto the interorbital region of the frontal). Moreover, character 47 (squamosal

794 dorsoventrally elongated) is also an exclusive synapomorphy of this clade.

795 Seventeen synapomorphies support the monophyly of Neobalaenidae + Balaenidae to the

796 exclusion of *Morenocetus parvus*. Three of them are unambiguous: characters 81 (short

797 dorsoventral height of the tympanic cavity), 82 (dorsoventrally compressed tympanic bulla), and

798 83 (enlargement of epitympanic hiatus). Characters 11 (rostrum highly arched), 84

799 (anteroposteriorly short anterolateral lobe of tympanic bulla), 92 (dorsal exposure of mandibular

800 condyle), 95 (dorsoventral arc of dentary along the whole length of the bone), and 101 (cervical

801 vertebrae fused) represent additional ambiguous synapomorphies of the clade. Neobalaenidae

802 (including *Caperea* and *Miocaperea*) is the sister-group of Balaenidae (here including *Balaena,*

803 *Balaenella, Balaenula* and *Eubalaena*). The monophyly of Neobalaenidae is supported by 4

804 synapomorphies including a reversal in character 122 (complete infundibulum). Characters 50

805 (presence of squamosal cleft) and 75 (exposure of posterior process of petrotympanics in the lateral

806 view of the skull) are ambiguous synapomorphies as these characters (in different ways) are

807 observed in Balaenopteridae and Cetotheriidae, presumably as a result of convergent evolution.

808 Four unambiguous synapomorphies support the monophyly of Balaenidae: characters 64 (massive

809 elongation of palatine posteriorly), 65 (posterior placement of pterygoid), 86 (sharply defined

810 groove for mylohyoidal muscle), and 122 (foramen ovale with incomplete infundibulum). Three

811 additional ambiguous synapomorphies are detected: characters 12 (transverse compression of

812 maxilla), 74 (long and thick roof of stylomastoid fossa), and 97 (strong anterior torsion of dentary).

813 Balaenidae is subdivided into two clades: one including *Balaena* and *Balaenella* and the other

814 including *Balaenula* and *Eubalaena*. The inclusion of *Balaenella brachyrhynus* within *Balaena*

815 casts some taxonomic problems as it either makes *Balaena* paraphyletic or suggests inclusion of

816 *Balaenella* within *Balaena*. *Balaenella brachyrhynus* and *Balaena montalionis* share an anteriorly

817 narrowed supraoccipital and a supraoccipital with transversely short anterior border; these

818 character states support their sister-group relationship. Unfortunately, a clear illustration of the

819 dorsal view of *Balaena ricei* is not available and it is difficult to understand whether this species

820 is really more closely related to *Balaena montalionis* and *Balaenella brachyrhynus* or to *Balaena*

821 *mysticetus*. From our results, *B. mysticetus* represents a separate lineage that diverged before the

822 other *Balaena*-like taxa (*B. ricei*, *B. montalionis* and *Balaenella*). A low number of

823 synapomorphies support the monophyly of the clade including *Balaena* and *Balaenella*. These

824 include the following two unambiguous synapomorphies: characters 116 (transverse compression

825 of anterior supraoccipital) and 120 (lateral projection of zygomatic process of the squamosal).

826 Additionally, two ambiguous synapomorphies are also found to support this clade; these include

827 characters 126 (posterior orientation of dorsoventrally developed squamosal body) and 132 (crest

828 present at parietal-squamosal suture). The sister-group relationship of *Balaena montalionis* and

829 *Balaenella brachyrhynus* is supported by one unambiguous synapomorphy (character 117: squared

830   anterior border of supraoccipital) and one ambiguous synapomorphy (character 118: short anterior

831   border of supraoccipital).

832

833   *Relationships of* Eubalaena

834   Confirming previously published hypotheses (Bisconti, 2000, 2005a; Churchill et al., 2012), our

835   analysis resulted in the monophyly of a clade including *Balaenula* and *Eubalaena* (Fig. 12). The

836   clade including *Eubalaena* and *Balaenula* is the sister-group to the *Balaena + Balaenella* clade.

837   *Balaenula* is the sister-group of *Eubalaena*. Three unambiguous and one ambiguous

838   synapomorphies support this clade. The unambiguous synapomorphies include characters 123

839   (transverse orientation of supraorbital process of the frontal in lateral view), 129 (curvature of

840   rostrum with horizontal proximal part), and 130 (concavity on the anterior border of nasal).

841   Character 118 (transversely wide anterior border of supraoccipital) was also found to support this

842   clade (ambiguous synapomorphy).

843   *Eubalaena shinshuensis* is the first *Eubalaena* species to branch; the *Eubalaena* sp. from the Late

844   Pliocene of Tuscany is the sister-group of the living *Eubalaena* species + *E. ianitrix* and its

845   inclusion on a separate ramus suggests that it could be a different *Eubalaena* species of its own.

846   *Eubalaena japonica* and *E. australis* branch before *E. ianitrix* and *E. glacialis*, the two latter being

847   sister-groups.

848   Only one unambiguous synapomorphy was found to support the monophyly of the right whale

849   genus *Eubalaena*; character 115 (presence of a dome on the supraoccipital). We think that this

850   reduced morphological support for the well-established *Eubalaena* genus is due to the fact that

851   most of the characters previously used to support its monophyly are shared with *Balaenula*.

852   *Eubalaena shinshuensis* from the Messinian of Japan was found to be the earliest-diverging right

853 whale species of the genus; the Pliocene *Eubalaena* sp. from Tuscany is the sister-group of the

854 living *Eubalaena* species + *E. ianitrix*. The monophyly of the *Eubalaena* sp. from Tuscany and

855 the crownward *Eubalaena* species was supported by one unambiguous synapomorphy (character

856 127: squared exoccipital in lateral view) and one ambiguous synapomorphy (character 126:

857 vertical orientation of squamosal body).

858 The clade including the living *Eubalaena* species and *E. ianitrix* is supported by 5 unambiguous

859 synapomorphies (125: parietal-frontal suture with distinctive anteroventral corner; 131: short

860 nasals; 133: parietal spreads on the supraorbital process of the frontal; 140: presence of vascular

861 groove on posterior part of pars cochlearis; and 141: evident pyramidal process posterior to

862 perilymphatic foramen) and 8 ambiguous synapomorphies (114: sagittal concavity on

863 supraoccipital; 134: anterior protrusion of parietal-squamosal suture; 135: prismatic posterior

864 process of petrosal; 138: transversely elongated pars cochlearis; 143: long transverse process of

865 the atlas; 146: highly concave anterior and posterior borders of humerus; 147: globular humeral

866 head; 150: superior corner of olecranon reduced-to-absent; and 151: reduced-to-absent coracoid

867 process in scapula) (Fig. 13).

868 *Eubalaena australis* was found to be more closely related to *E. ianitrix* + *E. glacialis* than *E.*

869 *japonica*. The sister-group relationship of *E. glacialis* with *E. ianitrix* + *E. glacialis* was supported

870 by two unambiguous synapomorphies: characters 139 (crista transversa exits from internal

871 acoustic meatus) and 152 (transverse orientation of tyrohyoidal processes). It is noticeable that

872 none of these characters is preserved in the holotype of *E. ianitrix* and the placement of this species

873 in this precise position in the cladogram relies on ACCTRAN optimization of the morphological

874 transformations operated by TNT. The monophyly of the clade *Eubalaena ianitrix* + *E. glacialis*

875   is supported by a single ambiguous synapomorphy: character 121 (presence of pterygoid in

876   temporal fossa).

877

878   *Stratigraphic Consistency Index*

879   The calculation of the Stratigraphic Consistency Index shows that the degree of agreement of the

880   branching pattern with the stratigraphic occurrence of the taxa is exceptionally high. The SCI

881   depends on (1) the number of well-resolved nodes and (2) the number of stratigraphically

882   consistent nodes. In the hypothesis of phylogeny presented in this paper, the maximum number of

883   nodes is 40 (number of OTUs minus 2) and the number of stratigraphically consistent nodes is 33.

884   The SCI is thus 0.825.

885

886   *Divergence dates of balaenoid clades*

887   In Fig. 14 the hypothesis of phylogeny for Balaenoidea proposed in the present paper is plotted

888   against the stratigraphic age of the included OTUs. In the Figure, branch lengths are inferred from

889   the phylogenetic relationships of the taxa and from the stratigraphic ages of the representative

890   fossil record of each OTU.

891   The age of *Miocaperea pulchra* suggests that the origin of the clade including Balaenidae +

892   Neobalaenidae is older than Tortonian (early Late Miocene). Unfortunately, given that

893   *Morenocetus parvus* falls outside Neobalaenidae + Balaenidae, it is not possible to be sure about

894   the precise age of origin of these families. Indeed, as the stratigraphic occurrence of *M. parvus* is

895   limited to the Burdigalian (late Early Miocene), the age of origin of Neobalaenidae and Balaenidae

896   may be constrained to a time interval between Burdigalian and Tortonian.

897   The fossil record of *Balaena*-like species does not extend before Zanclean (Early Pliocene). The

898   stratigraphic occurrences of *Balena montalionis*, *B. ricei* and *Balaenella brachyrhynus* suggest

899   that an expansion of the paleobiogeographic range of *Balaena*-like taxa was attained during the

900   earliest part of the Pliocene with invasion of Mediterranean, North Atlantic and North Sea. The

901   sister-group relationship of *Balaena mysticetus* and the other *Balaena*-like taxa suggest that the

902   direct ancestor of the living bowhead whale originated around the Zanclean or slightly earlier and

903   possibly quickly invaded the Arctic region, leaving us more limited possibilities to find fossil

904   records relevant for the morphological transition towards the extant species.

905   The stratigraphic age of *Eubalaena shinshuensis* is the most crucial point in the present

906   reconstruction of the divergence dates of balaenoid taxa. In fact, as the occurrence of this species

907   is from the Messinian, the origin of the whole *Balaenula + Eubalaena* clade must be traced back

908   to at least the latest Miocene. This means that the separation of the living right whales from their

909   closest living relative (i.e., *Balaena mysticetus*) is from 7-to-5.4 million years ago which

910   significantly increases the hypothesized divergence date based on McLeod et al. (1993) and

911   reduces to one-third of the hypothesized divergence date based on Bisconti (2005b) and Santangelo

912   et al. (2005). The impact of this new divergence date on the reconstruction of the demographic

913   history of the right whales based on genetic measures of diversity will be analysed elsewhere.

914   As far as the origins of the living *Eubalaena* species is concerned, the Messinian age of *E.*

915   *shinshuensis* suggests that the origin of the genus *Eubalaena* should be found at least in the latest

916   Miocene. The stratigraphic occurrences of the *Eubalaena* sp. from Tuscany and *E. ianitrix*

917   constrain the origin of the living right whale species to at least the Piacenzian. Therefore, we

918   estimate that the modern *Eubalaena* species originated in a period between 3.5 and 2.6 Ma. As we

919   will show in another paragraph, it is more difficult to determine a chronological placement for the

920 origin of the northern right whale *E. glacialis* because the origin of this species could be due to a

921 process of phyletic transformation from *E. ianitrix*, occurring in a time interval ranging from the

922 Piacenzian to the Pleistocene.

923 In summary, the stratigraphic distribution of the main evolutionary events of Balaenoidea are

924 presented in Fig. 13. Following our phylogenetic analysis and the computation of stratigraphic

925 ages of the included OTUs, the origin of Balaenoidea should be traced at least as far as the

926 Burdigalian (age of *Morenocetus parvus*). The origin of the living families (Neobalaenidae and

927 Balaenidae) occurred before the Tortonian (age of *Miocaperea pulchra*). The splitting between the

928 *Balaena*-like and the *Balaenula + Eubalaena* clades occurred before the Messinian (age of

929 *Eubalaena shinshuensis*). The origin of the modern *Eubalaena* radiation (including *E. ianitrix*)

930 dates at least from the Piacenzian. The separation between the living right whale species and their

931 extant relative (*Balaena*) dates at least from the earliest Messinian (*c.* 7 Ma).

932

933 **Discussion**

934

935 *Body size estimate*

936 The methods we used to estimate the size of *Eubalaena ianitrix* resulted in a total body length

937 included between 6 and 7 m and a body mass of *c.* 20 t. The statistical methods used have their

938 shortcomings in that most of them were not tested on species of the genus *Eubalaena*. The ratio

939 between skull length and body length is a general estimate of body proportions in Balaenidae used

940 by several authors based on observations of mounted skeletons, and killed and stranded animals

941 (Koshi et al., 1993; Tomilin, 1967; Omura, 1958). The ratio between supraoccipital length and

942 total skull length was used by Bisconti (2002) based on a small dataset of right whale

943   measurements and its correlation coefficient R^2 is rather low; therefore, the body size estimate

944   generated by this method must be considered as preliminary pending the inclusion of more

945   measurements in the dataset. However, all the methods used converge toward a total body length

946   of 6-to-7 m and we think that this result should be close to the true length of the living animal. At

947   present, we have no reason to suppose that a kind of systematic error occurred in a consistent

948   manner to provide a systematically wrong result based on all the methods used.

949   It is unclear whether this size represents the maximum length of *E. ianitrix* because nothing is

950   known about its individual variation. If compared with other balaenids, it represents a medium-

951   sized species (see Supplementary Table S2 and Supplementary Figure S1). More precisely, it is

952   the only medium-sized species within the *Eubalaena* clade (Supplementary Figure S2), suggesting

953   that its medium size is a derived condition. The origin of the size reduction in *E. ianitrix* may be

954   related to the warmer temperature of the southern portion of the North Sea during the deposition

955   of the Lillo Formation (latest Zanclean-early Piacenzian; Laga et al. 2006). In fact, the Kruisschans

956   Sands Member of the Lillo Formation (in which the holotye skull of *E. ianitrix* was found)

957   deposited in a shallow, low-energy environment, where molluscs indicate some degree of cooling,

958   but where the palynological assemblage suggests mild-temperate to warm marine conditions

959   (Marquet, 1993; Louwye et al., 2004; De Schepper et al., 2009). However, it is still unknown

960   whether *E. ianitrix* inhabited permanently the southern North Sea.

961   In the extant *Eubalaena glacialis* and *E. australis*, a total body length of less than 7 m corresponds

962   to the length of individuals less than one year old (George et al. 2016; Fortune et al. 2012). The

963   holotype skull of *Eubalaena ianitrix*, however, shows sutural morphologies and general robustness

964   inconsistent with the general osteological features of newborn and early juvenile individuals (e.g.,

965   occipital joints not closed, presence of spongy bone; see Walsh & Berta, 2011). Rather, its robust

966   muscular attachments on the supraoccipital and the degree of fusion at the frontoparietal (coronal)

967   and parietal-squamosal sutures suggests that its age was older than 1 year. It is impossible to assess

968   at which stage of its life cycle it died as nothing is known about intraspecific variation in skull and

969   body length in *E. ianitrix*. Future discoveries of new specimens from different age classes will help

970   providing an overview of the ontogenetic variation in body size in this newly discovered species.

971   The estimate of the body mass obtained in the present work is at odds with published records

972   regarding the relationships of body mass and total body length in extant Balaenidae. Fortune et al.

973   (2012) reported weights ranging from 0.7 to 11 t for 6-9 m long bowhead whales, while Trites &

974   Pauli (1998) estimated masses ranging from 19 to 24 t for 16-18 m long northern and southern

975   right whales. Our result of *c.* 20 for the 6-7 m long *Eubalaena ianitrix* appears overestimated,

976   suggesting that more research is needed to develop more accurate statistical methods for inferring

977   body size and body mass information in Balaenidae.

978

979   *Phylogeny: Relationships of Balaenidae*

980   Phylogenetic analyses of Balaenidae were published by several authors in the last 25 years.

981   McLeod et al. (1993) were the first to publish a phylogenetic tree based on manual manipulation

982   of morphological character states. They found a monophyletic Balaenoidea and a sister group

983   relationship between Neobalaenidae and a clade formed by Balaenidae and Eschrichtiidae. The

984   sister-group relationship of Balaenidae and Eschrichtiidae was not confirmed by subsequent

985   phylogenetic works.

986   Bisconti (2000) performed the first computer-assisted cladistic analysis of Balaenidae, retrieving

987   a monophyletic Balaenoidea and a monophyletic Balaenidae. Within Balaenidae, Bisconti (2000)

988   found two different clades: one including the genus *Balaena* and the other including *Eubalaena*,

989 *Balaenula* and *Morenocetus*. After a substantial re-discussion of the fossil record of Balaenidae

990 (Bisconti, 2003) and of previously published phylogenetic analyses, Bisconti (2005a) published a

991 new phylogenetic analysis resulting in a monophyletic Balaenoidea and a monophyletic

992 Balaenidae; two clades were recovered in Balaenidae: one included *Morenocetus*, *Balaenella* and

993 *Balaena* and the other included *Eubalaena* and *Balaenula*. These finds were substantially

994 confirmed by Churchill et al. (2012) after an extensive reanalysis of the morphological evidence

995 of the phylogeny of Balaenidae.

996 Numerous other works on the phylogeny of mysticetes were published in the last decades that

997 included balaenids, but not explicitly focused on Balaenidae. However, it is important to consider

998 these works as they provide information about the sister-group relationships of Balaenidae and

999 other mysticete taxa. While most of the morphology-based works agree that Balaenidae and

1000 Neobalaenidae are sister-groups (Bisconti, 2015 and literature therein; Boessenecker & Fordyce,

1001 2016), several recent papers did not support the monophyly of Balaenoidea with Neobalaenidae as

1002 sister group of Balaenopteroidea (see Gol'din et al., 2014 and literature therein) or as part of

1003 Cetotheriidae (e.g., Marx & Fordyce, 2015 and literature therein). The placement of *Caperea*

1004 *marginata* and *Miocaperea pulchra* within Cetotheriidae depended upon peculiar treatments of

1005 some characters related to the shape and orientation of the squamosal, the elongation of the

1006 supraoccipital and the reduction of the ascending process of the maxilla. Criticisms to this

1007 approach were published by El Adli et al. (2014) and Bisconti (2015) suggesting that the Marx &

1008 Fordyce (2015) dataset should be revised. Marx & Fordyce (2016) provided a subsequent version

1009 of such a dataset that shows substantially the same characteristics, as it does not include character

1010 states describing the topological relationships of the bones forming the skull vault in Balaenidae

1011 and Neobalaenidae. The proposed sister-group relationship of Neobalaenidae and

1012 Balaenopteroidea + Cetotheriidae depends on (1) inclusion of molecular data or (2) emphasis on

1013 rorqual-like characters observed in *Caperea marginata* (i.e., long forelimb, presence of dorsal fin,

1014 and presence of ventral throat grooves).

1015 The problem of using molecular data to infer the phylogenetic relationships of clades mainly

1016 formed by fossil taxa (e.g., Hominidae, Mysticeti) has been addressed by several authors and this

1017 is the precise case of mysticetes where most of the described species are now extinct and cannot

1018 be used for DNA sequencing and analysis. Even if molecular analyses may include thousands of

1019 character states (base pairs from DNA sequences), the lack of data from most of the taxa belonging

1020 into the clade may be a serious problem as an enormous number of character states cannot be

1021 scored and must be inferred by the computer program used for the analysis. The accuracy of

1022 phylogenetic reconstructions based on molecular data for clades mainly formed by extinct taxa

1023 tends to be lower than that based on morphological data (Heath et al., 2008; Wagner, 2000). This

1024 suggests that emphasis should be given to morphological rather than molecular data in the

1025 inference of the phylogeny of mysticetes.

1026 Aside from that, it must be said that taxonomic uncertainties, problems with character descriptions

1027 and coding, and the discovery of large amounts of homoplasy in morphological datasets have

1028 plagued morphological attempts to infer phylogenetic relationships in mysticetes in the last twenty

1029 years (Deméré et al., 2005; Bisconti, 2007). Our effort to reduce dataset homoplasy was successful

1030 only in part. In fact, after the exclusion of evident homoplastic characters from our morphological

1031 dataset, the number of usable character states dropped down and our morphological evidence could

1032 provide only strong support for only some clades. Most of the species-level sister group

1033 relationships are thus supported by reduced numbers of synapomorphies. In this sense, what we

1034 observe in balaenid phylogenetics resembles what was observed in complicated analyses of

1035   evolutionary radiations occurring in relatively recent times (e.g., cichlid fishes and hominins; e.g.,

1036   Seehausen, 2006; Haile-Selassie et al., 2016) with the important difference that the evolutionary

1037   radiation of Balaenidae occurred in a longer time interval. However, studies of DNA substitution

1038   rates interestingly showed that mysticete DNA evolves much more slowly than that of other

1039   mammals (Rooney et al., 2001); therefore, only limited morphological change should be expected

1040   to occur in this group in the last few million years. This expectation is somewhat confirmed by the

1041   substantial stasis detected in the last 10 million years of neobalaenid evolution (Tsai & Fordyce,

1042   2015; Bisconti, 2012) and by the small amount of morphological diversity observed in Balaenidae

1043   as discussed in this work. The reasons of the slow evolutionary pace in Balaenidae are not

1044   completely understood; one character that could be correlated is the evolution of increased

1045   individual longevity, demonstrated to be linked to DNA preservation (Jackson et al., 2009; Keane

1046   et al., 2015), which, in its turn, should reduce the accumulation of mutations preventing the

1047   evolution of phenotypic diversity.

1048

1049   *Phylogeny: intra-family relationships within Balaenidae*

1050   Published studies specifically directed at discovering phylogenetic relationships of Balaenidae

1051   recently converged towards the subdivision of this family into two sub-clades: a clade including

1052   *Balaena* and *Balaenella* and a clade including *Balaenula* and *Eubalaena*. These two groups are

1053   well supported by morphological characters and correspond to two different skull structures (as

1054   evidenced by Miller, 1923; Kellogg, 1928; McLeod et al., 1993; Bisconti, 2005a).

1055   The contribution of the postcranial skeleton to the support for these clades is rather scanty but, for

1056   the first time, we detected that: (1) the dorsal transverse process of the atlas is dorsoventrally

1057   enlarged in *Eubalaena* and reduced in *Balaena* (including *B. mysticetus* and *B. ricei*), (2) the

1058 ventral transverse process of the atlas is long and forms a ventral corner in *Balaena* but is short

1059 and squared in *Eubalaena*, (3) the humerus is long and slender in *Balaena* while in *Eubalaena* it

1060 is shorter and with a more globular head, and (4) the dorsal corner of the olecranon process of the

1061 ulna is conspicuous in *Balaena* but reduced to absent in *Eubalaena*.

1062 The four characters outlined above could be useful to suggest phylogenetic and taxonomic

1063 affinities of fossils of uncertain position because of their poor preservation. This is the case of a

1064 number of partial skeletons from the Pliocene of Italy (Bisconti, 2003; Chicchi & Bisconti, 2014;

1065 Cioppi, 2014; Bisconti & Francou, 2014; Manganelli & Benocci, 2014; Sarti & Lanzetti, 2014)

1066 that should be reassessed based on this new evidence.

1067 As mentioned above, the sister-group relationship of *Balaena montalionis* and *Balaenella*

1068 *brachyrhynus* raises particular problems as the inclusion of *Balaenella* within *Balaena* would

1069 either make the latter paraphyletic, or would imply the assignment of *Balaenella* to *Balaena*.

1070 However, we feel that it is premature to choose one of the above options, as some morphological

1071 data from *Balaena ricei* were not available for this study (i.e., precise sutural pattern between

1072 parietal and frontal and between parietal and squamosal, and shape of the anterior end of the

1073 supraoccipital); this makes relationships within the *Balaena*-like subclade still biased by some

1074 uncertainty. However, the close relationship of *B. montalionis* and *B.lla brachyrhynus* seems well

1075 supported by the shared squared anterior border of the supraoccipital and the transverse

1076 compression observed in the anterior half of the lateral borders of the supraoccipital. The point,

1077 here, consists in understanding if *Balaena ricei* is more closely related to *Balaena mysticetus* or to

1078 the *B. montalionis* + *B.lla brachyrhynus* pair; more data are needed about the morphology of *B.*

1079 *ricei* to solve this question.

1080 Among right whales, *Eubalaena shinshuensis* is the first to branch off, due to the primitive sutural

1081 pattern observed in the skull of this Messinian species; the following branch is occupied by the

1082 Piacenzian *Eubalaena* sp. from Tuscany, due to the plesiomorphic parietal-squamosal suture and

1083 to a peculiar supraoccipital morphology. More interesting are the relationships of the living

1084 *Eubalaena* species and *E. ianitrix*. From our work, *E. japonica* is the earliest-diverging species

1085 among the living right whales, with *E. australis* and *E. glacialis* more closely related to each other.

1086 This result contradicts molecular studies that suggested that *E. australis* diverged earlier and that

1087 *E. glacialis* and *E. japonica* are sister-groups (e.g., Gaines et al., 2005; Rosenbaum et al., 2000).

1088 Also the DNA-based phylogeny of species of lices parasitizing living *Eubalaena* species lends

1089 support to the molecular hypothesis of relationships for right whales (e.g., Kaliszewska et al.,

1090 2005) thus suggesting that *E. glacialis* is the earliest-diverging *Eubalaena* species. However, these

1091 analyses did not include data from fossil right whales such as *E. shinshuensis*, *E. ianitrix*, and the

1092 *Eubalaena* sp. from Tuscany and did not take into account the fossil histories of the different lice

1093 species; therefore, they could be unable to retrieve correct results (in accordance with Heath et al.,

1094 2008; Wagner, 2000). Moreover, assuming an early branching of *E. glacialis* in the phylogeny of

1095 the living right whales implies that reticulate biogeographic histories have occurred between the

1096 southern and the North Pacific *Eubalaena* species to account for the peculiar genetic patterns

1097 observed in cyamid lices (Kaliszewska et al., 2005).

1098

1099 *Divergences of the living right whale species*

1100 Divergence ages of living balaenid species are important for the reconstructions of the

1101 demographic histories of these taxa in the context of conservation biology. Divergence dates are

1102 used in equations dealing with the genetic diversity of the living populations to assess whether

1103   living species suffered of genetic bottlenecks due to environmental change or human impact (e.g.,

1104   Rosenbaum et al., 2001). Fossil calibrations of divergence dates are necessary to constrain the pace

1105   of molecular clocks in order to get correct results in terms of assessments of genetic diversity and

1106   evolution (Quental & Marshall, 2010).

1107   Several works have provided estimates of divergence ages of balaenid species. McLeod et al.

1108   (1993) suggested a separation date between *Eubalaena* and *Balaena* of *c.* 4.5 Ma based on analysis

1109   of the balaenid fossil record. This assessment was used by Rosenbaum et al. (2001) to analyse the

1110   genetic diversity of the living bowhead whale, *Balaena mysticetus*, with the conclusion that this

1111   species did not suffer of population bottlenecks due to human whaling activities. Bisconti (2005b)

1112   and Santangelo et al. (2005) questioned this conclusion based on the phylogenetic analysis

1113   provided by Bisconti (2005a); the latter opened the possibility that the divergence between

1114   *Eubalaena* and *Balaena* occurred in the Early Miocene. This conclusion resulted from the

1115   placement of *Morenocetus parvus* as sister-group of the *Balaena*-like subclade to the exclusion of

1116   the *Balaenula + Eubalaena* subclade (Bisconti 2005a) thus providing a divergence date of *Balaena*

1117   and *Eubalaena* of more than 20 Ma.

1118   Subsequent analyses did not confirm this result as molecule-based and morphology-based works

1119   suggested later divergence dates (e.g., Sasaki et al., 2007; Churchill et al., 2012) and placed the

1120   divergence of *Balaena* and *Eubalaena* in a time interval ranging from *c.* 4 to *c.* 7 Ma. The

1121   phylogenetic analysis of *Cyamus* lices confirms a divergence at *c.* 6.6 Ma for the living right whale

1122   and bowhead whale species (Kaliszewska et al., 2005).

1123   The phylogenetic analysis of the present work (Figs 12 and14) reinforces a minimum late Miocene

1124   divergence (Messinian: *c.* 7-5.4 Ma) based on the age of the earliest diverging *Eubalaena* species

1125   (i.e., *E. shinshuensis*). In fact, an earlier divergence age is not unlikely, considering that (1) based

1126   on the present work, the separation between Balaenidae and Neobalaenidae dates from at least the

1127   Tortonian (*c.* 10 Ma) and (2) the separation of the *Balaena*-like subclade from the *Balaenula* +

1128   *Eubalaena* subclade is deep in time and originates from the very origin of Balaenidae (Bisconti,

1129   2005a; Churchill et al., 2012; this work).

1130   How the reconstructions of the demographic histories of balaenids will be impacted by a Late

1131   Miocene age of divergence between *Eubalaena* and *Balaena* is outside the scope of the present

1132   paper. However, we suggest here that the past estimates of genetic diversity in right and bowhead

1133   whale populations should be considered with caution as those were based on underestimated

1134   (McLeod et al., 1993) or overestimated (Bisconti, 2005b; Santangelo et al., 2005) divergence ages.

1135

1136   *Possible ancestor-descendant relationships between* Eubalaena ianitrix *and* Eubalaena glacialis

1137   There is not a commonly accepted method to infer ancestor-descendant relationships (ADRs) in

1138   phylogenetics as it is supposed that only in exceptional cases such a relationship can be detected

1139   in the fossil record (Paul, 1992). The most usual recommendation to those who try to recover ADR

1140   from the fossil record consists in being sure that a reasonably complete sample is available for the

1141   past diversity of the investigated group. While it is certain that this is not the case for fossil

1142   cetaceans, some attempts to reconstruct ADRs in this order were attempted in the past with a

1143   diversified array of methods.

1144   Uhen & Gingerich (2001) provided an ADR for *Chrysocetus healyorum* and Neoceti (Mysticeti +

1145   Odontoceti). They used a stratocladistic approach in three steps: (1) they performed a traditional

1146   computer-assisted, morphology-based cladistics analysis retrieving a set of resulting cladograms;

1147   (2) they added a stratigraphic character and manipulated the initial hypothesis of relationships by

1148   hand in order to explore whether *C. healyorum* could be the direct ancestor of Neoceti; (3) they

1149   calculated a new set of cladograms via a computer-assisted algorithm. They found one most

1150   parsimonious tree in which *C. healyorum* was placed as direct ancestor of Neoceti. In the

1151   subsequent discussion, they suggested that newly discovered advanced archaeocete taxa could fit

1152   the ancestor position for Neoceti in a better way than *C. healyorum* thus giving this taxon a

1153   temporary ancestor status.

1154   More recently, Tsai & Fordyce (2015) suggested an ADR for *Miocaperea pulchra* and *Caperea*

1155   *marginata* based on a combination of cladistic analysis of traditional OTUs + juvenile individuals

1156   of *C. marginata* and by providing a discussion on the impact of the morphology of juvenile

1157   characters in phylogeny reconstruction. Apart from cetaceans, ADR were also hypothesized for

1158   the fur seal *Callorhinus* (Boessenecker 2011), great white sharks (Ehret et al. 2012), and the

1159   dinosaur *Triceratops* (Scannella et al. 2014)

1160   All of these methods have their own merits and shortcomings; Uhen & Gingerich (2001) realized

1161   a systematized search for the most parsimonious solutions but their results were limited by

1162   uncertainties about the completeness of the relevant fossil record; Tsai & Fordyce (2015) used data

1163   from a hotly debated source of data (i.e., juvenile and embryonic specimens) (e.g., Hall, 1996 and

1164   literature therein). Apart from that, however, the search for ADRs is always worth doing, as it

1165   potentially gives information on natural evolutionary processes.

1166   Here, we suggest that an ADR should be proposed for the *Eubalaena ianitrix* and *Eubalaena*

1167   *glacialis* species pair. We support our hypothesis of relationships based on what follows:

1168   (1) *E. glacialis* and *E. ianitrix* are phylogenetically more closely related than all the other

1169   species belonging to *Eubalaena*; they share one peculiar synapomorphy that is not

1170   observed in any other *Eubalaena* species (i.e., presence of the pterygoid in the temporal

1171   fossa).

(2) Molecular studies suggest that the branch of *E. glacialis* has been separated from the other living right whale species for a long time (up to 3 million years). This long time interval excludes the possibility of an arrival in the North Atlantic due to a Plesistocene or Holocene invasion from the North Pacific or the southern right whale species (Kaliszewska et al., 2005). Thus, it is highly likely that *E. glacialis* originated in that portion of the northern hemisphere that includes the North Atlantic and the North Sea.

(3) *E. glacialis* and *E. ianitrix* share part of their geographic distribution. Even if only one specimen of *E. ianitrix* is known up to now, its geographic occurrence is included within the geographic range of *E. glacialis*.

(4) The geographic area that encompasses the distribution of *E. ianitrix* and *E. glacialis* underwent extensive environmental change during the past 1.5 million years (Zachos et al., 2001), supporting the hypothesis that selective regimes could have been active there implying phenotypic evolution in previously established populations. In particular, the temperature decline observed in the whole northern hemisphere during the Pleistocene could have been the driver of organismal responses that can be described (in part, at least) by the Bergmann's rule (i.e., increasing body size).

(5) Assuming a species longevity of 2 million years (Fordyce & de Muizon, 2001; Steeman et al., 2009), and hypothesizing that *Eubalaena glacialis* became a well-defined species around the Pliocene-Pleistocene boundary, there may be a time interval in which *E. ianitrix* and the earliest individuals of *E. glacialis* co-occurred in the same area where the morphological transition happened. Unfortunately, the estimated species longevity mentioned above is only based on the observation that the fossil record of the living mysticete species does not exceed *c.* 2 million years (Fordyce, 2002). Based on molecular

1195   data, alternative analyses suggest longer species durations (see Pastene et al. 2007 for

1196   *Balaenoptera acutorostrata* and Sasaki et al. 2005 for many species of baleen-bearing

1197   whales; these studies suggest divergence dates of some living species exceeding 2 million

1198   years). This does not contradict our proposed sympatry hypothesis for *E. glacialis* and *E.*

1199   *ianitrix*; rather, hypothesizing longer species duration would reinforce this hypothesis. To

1200   our knowledge, no molecule-based work supports a species duration shorter than 2 million

1201   years for extant baleen-bearing whales.

1202   (6) Bearing in mind the paleoenvironmental changes that occurred in the northern hemisphere

1203   from the earliest Pleistocene (*c.* 2.6 Ma) through most of that epoch, a transformation of a

1204   previously established population of right whale into a more ecologically-optimized

1205   species is a reasonable hypothesis.

1206   (7) From a skeletal morphology perspective, if a phyletic transformation of *E. ianitrix* into *E.*

1207   *glacialis* occurred, then it involved: (i) massive size increase at adulthood enabling the

1208   extant *E. glacialis* to reach more than 20 m in length at maturity (Tomilin, 1967) against

1209   the *c.* 7 m of *E. ianitrix* (consistent with Bergmann's rule in a colder environment), (ii)

1210   possible allometric adjustments of bone proportions (this is a direct consequence of point

1211   1), (iii) loss of the crest at the parietal-squamosal-supraoccipital suture, and (iv) change in

1212   the orientation of the posteromedial corner of the palatine. The crest at parietal-squamosal-

1213   supraoccipital suture appears to have been lost in the common ancestor of *E. glacialis* + *E.*

1214   *ianitrix* + *E. japonica* + *E. australis* clade and its presence in *E. ianitrix* is to be interpreted

1215   as a reversal to a plesiomorphic condition. The same applies to the protrusion of the

1216   posteromedial corner of the palatine. The recurrent evolution of these two characters

1217   suggests that some homoplasy occurred in the above clade in the last few million years.

1218   (8) Current genetic evidence supports the view that three distinct species of right whales

1219   inhabit three different ocean basins (Malik et al., 2000; Rosenbaum et al., 2001):

1220   *Eubalaena glacialis* in the North Atlantic and adjacent waters, *E. japonica* in the North

1221   Pacific, and *E. australis* in the Southern Ocean. Balaenoid whales perform a particular

1222   feeding behavior directed at capturing calanoid copepods; this feeding behavior is known

1223   as continuous ram feeing (Sanderson & Wassersug, 1993) or skim feeding (Pivorunas,

1224   1979). In the northern hemisphere, there is a geographic separation between the skim

1225   feeding species: the bowhead whale inhabits Arctic waters, while the right whales inhabit

1226   more temperate waters and the two right whale species of the northern hemisphere are

1227   separated by the Eurasia and thus do not compete for food or reproductive areas. In the

1228   southern hemisphere, the two skim feeding species are geographically separated as the

1229   southern right whale feeds around Antarctica while the pygmy right whale is restricted to

1230   more temperate waters; apparently, there is no competition between these species for food

1231   or reproductive areas. It appears, thus, that only one skim feeding species is "allowed" to

1232   live in a given ocean basin, and we may hypothesize that the pattern was not different in

1233   the past million years. For this reason, we may expect that only one or a few right whale

1234   species occupied a given geographic area in time intervals of *c*. 2 million years (mean

1235   duration of a marine mammal species; see above). This suggests that, paradoxically, the

1236   taxonomic sample of the right whale diversity in the Late Pliocene of the northern

1237   hemisphere is rather complete. This inference is also confirmed by the high value of the

1238   SCI obtained here, suggesting that most of the phylogenetic relationships presented here

1239   can be explained without the need for long ghost lineages. This inference fills the requests

1240   for a dense taxonomic sampling in the taxa under investigation and allows us to give further

1241   support to our hypothesis of ADR for *Eubalaena ianitrix* and *E. glacialis*. It must be said,

1242   however, that the current diversity of right and bowhead whales includes only large-sized

1243   species, whereas, in the Pliocene, large-sized and small-sized balaenid species are

1244   demonstrated to have been sympatric (Bisconti, 2003). Moreover, several studies have

1245   addressed the impact of shark predation on Pliocene right whales, suggesting some

1246   differences in the trophic webs of the Pliocene oceanic basins with respect to modern times.

1247   The ecological meanings of these differences are still not fully understood, potentially

1248   impacting our hypothesis regarding the taxonomic completeness of the balaenid fossil

1249   record.

1250   (9) In a way to test the ADR for *Eubalaena ianitrix* and *E. glacialis*, we followed the

1251   stratocladistic approach of Uhen & Gingerich (2001). The taxon x character matrix and the

1252   single most parsimonious tree were taken to MacClade (Maddison & Maddison, 2000).

1253   First, without the addition of a stratigraphic character, the ADR for *E. ianitrix* and *E.*

1254   *glacialis* was demonstrated to increase the tree length of two steps, as compared to the

1255   original tree length with a sister-group relationship. After addition of the stratigraphic

1256   character (see Supplementary Information) and without any other modification of the

1257   topology, the difference in tree length decreased from two steps to one step, meaning that

1258   the sister-group relationship was still the most parsimonious, but that stratigraphic data,

1259   namely the Piacenzian age of *E. ianitrix*, made the difference less significant. Swapping

1260   branches by hand, ADR for *E. ianitrix* and *E. glacialis* was found more parsimonious than

1261   a sister-group relationship only with (i) *E. shinshuensis* being more stemward than

1262   *Balaenula astensis*, and (ii) the three extant *Eubalaena* species forming a clade, with *E.*

1263   *ianitrix* as their last common ancestor. The need for such changes in topology may indicate

1264   that *E. ianitrix* is not the ancestor of *E. glacialis*. However, we think that such a pattern is

1265   strongly impacted by the scanty Pliocene balaenid fossil record in some areas (for example

1266   the North Pacific and the Southern Ocean). Pending the future discovery of fossil relatives

1267   of *E. australis* and *E. japonica*, stratocladistic analyses will most likely not be able to

1268   unambiguously discriminate ADR and sister-group relationships for *E. ianitrix* and *E.*

1269   *glacialis*.

1270

1271 **Conclusions**

1272

1273 We re-described specimens previously referred to *'Balaena' belgica* and found what follows.

1274   (1) The cervical complex RBINS M. 881 (IG 8444) that was originally designated as type of

1275   *'Balaena belgica* by Abel (1941) is poorly preserved and does not show diagnostic

1276   characters below the family level; therefore, we assign it to Balaenidae gen. et sp. indet.;

1277   this decision makes *'Balaena' belgica*, and its recombination nomina dubia.

1278   (2) The fragment of maxilla RBINS M. 880 lacks crucial diagnostic characters and cannot be

1279   assigned to any of the described balaenid genera and species; it is therefore assigned to

1280   Balaenidae gen. et sp. indet.

1281   (3) The morphology of the humerus RBINS M. 2280 is closer to that of *Eubalaena glacialis*

1282   as compared to *Balaena mysticetus* in the shape of the articular facet for the olecranon

1283   process of the ulna, in the overall shape of the deltoid tuberosity, and in the shape of the

1284   posterior border of the diaphysis. However, it differs from *E. glacialis* and other extant

1285   *Eubalaena* species in the elongation of the straight posterior border of the diaphysis; it is

1286   therefore assigned to *Eubalaena* sp. indet. This humerus corresponds to a large individual

1287   reaching a total body length over 16.5 m; it represents the first report of a gigantic right

1288   whale in the fossil record of the North Sea.

1289 (4) The neurocranium RBINS M. 879a-f represents the holotype of the new species *Eubalaena*

1290   *ianitrix*. This species is described and analysed into a phylogenetic context. From a

1291   morphological viewpoint, *E. ianitrix* is very close to the northern right whale *E. glacialis*

1292   in having the same sutural pattern in the skull vault and in sharing the presence of pterygoid

1293   in the temporal fossa. From a phylogenetic view, *E. ianitrix* is the sister-group of *E.*

1294   *glacialis*.

1295 (5) Our phylogenetic analysis also retrieved a monophyletic Balaenoidea, with *Morenocetus*

1296   *parvus* as the earliest stem balaenoid taxon, and with Neobalaenidae being the sister-group

1297   of Balaenidae. Two clades are observed within Balaenidae: one including *Balaena*-like

1298   taxa (genera *Balaena* and *Balaenella*) and the other including *Balaenula* and *Eubalaena*.

1299   The Messinian *E. shinshuensis* is the earliest diverging *Eubalaena* species; the *Eubalaena*

1300   sp. from Tuscany is the sister-group of a clade including all the living *Eubalaena* species

1301   and *E. ianitrix*.

1302 (6) The separation of *Eubalaena* from *Balaena* is estimated to have occurred around 7 Ma

1303   (minimum age). The origins of the living right whale species should be chronologically

1304   constrained to the Piacenzian (Late Pliocene: at least between 3.6 and 2.6 ma). Judging

1305   from supporting synapomorphies, stratigraphic ranges and ecological requirements, it is

1306   suggested that *Eubalaena ianitrix* is the direct ancestor of *E. glacialis*, the latter is proposed

1307   to have evolved via phyletic transformation, through body size increase and allometric

1308   adjustments during the temperature decline of the latest Pliocene and Pleistocene.

1309

1310 *Acknowledgments*

1311 The authors wish to thank Annelise Folie, Alain Drèze and Cécilia Cousin (all at RBINS, Brussels)

1312 for providing access to the specimens and for assisting in the transport of these heavy bones;

1313 Stéphane Berton and Marc Spolspoel (both at RBINS, Brussels) for their help when restoring the

1314 specimens studied here and when taking photos of part of the specimens illustrated here,

1315 respectively. Many thanks are due to Richard Monk, Eric Brothers, Eileen Westwig, Maria

1316 Dickson, and Nancy Simmons (all at AMNH, New York), Graham and Margaret Avery and

1317 Leonard Compagno (all at IZIKO, Cape Town), Reinier Van Zelst, John De Vos, Steven Van Der

1318 Mije and Wendy Van Bohemen (all at Naturalis, Rotterdam) for granting access to specimens

1319 under their care. Many thanks are due to Mark D. Uhen (George Mason University, Fairfax),

1320 Robert W. Boessenecker (College of Charleston) and J.G.M. Thewissen (PeerJ editor) for their

1321 reviews that highly enhanced the quality and the clarity of the manuscript.

1322

1323 References

1324

1325 Abel O. 1941. Vorläufige Mitteilungen über die Revision der fossilen Mystacoceten aus dem

1326 Tertiär Belgiens. *Bulletin du Museum Royal d'Histoire Naturelles de Belgique* 24(17):1–29.

1327 Benke H. 1993. Investigations on the osteology and the functional morphology of the flipper of

1328 whales and dolphins (Cetacea). *Investigations on Cetacea* 24:9–252.

1329 Bisconti M. 2000. New description, character analysis and preliminary phyletic assessment of two

1330 Balaenidae skulls from the Italian Pliocene. *Palaeontographia Italica* 87:37–66.

1331 Bisconti M. 2002. An early late Pliocene right whale (Genus *Eubalaena*) from Tuscany (Central

1332 Italy). *Bollettino della Società Paleontologica Italiana* 4:83–91.

1333   Bisconti M. 2003. Evolutionary history of Balaenidae. *Cranium* 20:9–50.

1334   Bisconti M. 2005a. Morphology and phylogenetic relationships of a new diminutive balaenid from

1335   the lower Pliocene of Belgium. *Palaeontology* 48:793–816.

1336   Bisconti M. 2005b. Paleontologia e conservazione: il caso della balena della Groenlandia. Pp. 133–

1337   142 in Scapini F. (ed.), La logica dell'evoluzione dei viventi – Spunti di Riflessione. Atti del

1338   XII Convegno del Gruppo Italiano di Biologia Evoluzionistica. Firenze University Press,

1339   Firenze, 167 pp.

1340   Bisconti M. 2007. A new basal balaenopterid from the Early Pliocene of northern Italy.

1341   *Palaeontology* 50:1103–1122.

1342   Bisconti M. 2008. Morphology and phylogenetic relationships of a new eschrichtiid genus

1343   (Cetacea: Mysticeti) from the Early Pliocene of northern Italy. *Zoological Journal of the*

1344   *Linnean Society* 153:161–186.

1345   Bisconti M. 2011. New description of *'Megaptera' hubachi* Dathe, 1983 based on the holotype

1346   skeleton held in the Museum für Naturkunde, Berlin. In: Bisconti M, Roselli A, Borzatti de

1347   Loewenstern A, eds. *Climatic Change, Biodiversity, Evolution: Natural History Museum*

1348   *and Scientific Research. Proceedings of the Meeting. Quaderni del Museo di Storia Naturale*

1349   *di Livorno* 23:37–68.

1350   Bisconti M. 2012. Comparative osteology and phylogenetic relationships of *Miocaperea pulchra*,

1351   the first fossil pygmy right whale genus and species (Cetacea, Mysticeti, Neobalaenidae).

1352   *Zoological Journal of the Linnean Society* 166:876–911.

1353   Bisconti M. 2015. Anatomy of a new cetotheriid genus and species from the Miocene of Herentals,

1354   Belgium, and the phylogenetic and paleobiogeographic relationships of Cetotheriidae s.s.

1355   (Mammalia, Cetacea, Mysticeti). *Journal of Systematic Palaeontology* 13:377–395.

1356   Bisconti M, Bosselaers M. 2016. *Fragilicetus velponi*: a new mysticete genus and species and its

1357   implications for the origin of Balaenopteridae (Mammalia, Cetacea, Mysticeti). *Zoological*

1358   *Journal of the Linnean Society* 177:450–474.

1359   Bisconti M, Francou C. 2014. I cetacei fossili conservati presso il Museo Geologico di

1360   Castell'Arquato (PC). *Museologia Scientifica Memorie* 13:31–36.

1361   Bisconti M, Lambert O, Bosselaers M. 2013. Taxonomic revision of *Isocetus depawi* (Mammalia,

1362   Cetacea, Mysticeti) and the phylogenetic relationships of archaic 'cetothere' mysticetes.

1363   *Palaeontology* 56:95–127.

1364   Boessenecker R. 2011. New records of the fur seal *Callorhinus* (Carnivora: Otariidae) from the

1365   Plio-Pleistocene Rio Dell Formation of Northern California and comments on otariid dental

1366   evolution. *Journal of Vertebrate Paleontology* 31:454-467.

1367   Boessenecker R. 2013. A new marine vertebrate assemblage from the Late Neogene Purisima

1368   Formation in Central California, part II: Pinnipeds and Cetaceans. *Geodiversitas* 35:815-940.

1369   Boessenecker R, Fordyce RE. 2016. A new eomysticetid from the Oligocene Kokoamu Greensand

1370   of New Zealand and a review of the Eomysticetidae (Mammalia, Cetacea). *Journal of*

1371   *Systematic Palaeontology*. DOI: http://dx.doi.org/10.1080/14772019.2016.1191045.

1372   Boessenecker RW, Fordyce RE. 2015. A new genus and species of eomysticetid (Cetacea:

1373   Mysticeti) and a reinterpretation of *'Mauicetus' lophocephalus* Marples, 1956: transitional

1374   baleen whales from the Upper Oligocene of New Zealand. *Zoological Journal of the Linnean*

1375   *Society*. DOI: 10.1111/zoj.12297.

1376   Brisson AD. 1762. *Regnum animale in classes IX Distributum, sive synopsis methodica*. Leiden:

1377   Theodorum Haak.

1378 Chicchi S, Bisconti M. 2014. Valentina, una balena fossile nelle collezioni dei Musei Civici di
1379   Reggio Emilia. *Museologia Scientifica Memorie* 13:54–55.

1380 Churchill M, Berta A, Deméré TD. 2012. The systematics of right whales (Mysticeti: Balaenidae).
1381   *Marine Mammal Science* 28:497–521.

1382 Churchill M, Clementz MT, Kohno N. 2014. Predictive equations for the estimation of body size
1383   in seals and sea lions (Carnivora: Pinnipedia). *Journal of Anatomy* 225:232–245.

1384 Cioppi E. 2014. I cetacei fossili a Firenze, una storia lunga più di 250 anni. *Museologia Scientifica*
1385   *Memorie* 13:81–89.

1386 Clapham PJ, Young SB, Brownell RL Jr. 1999. Baleen whales: conservation issues and the status
1387   of the most endangered populations. *Mammal Review* 29:35–60.

1388 Cope ED. 1891. *Syllabus of Lectures on Geology and Paleontology*. Philadelphia: Ferris Brothers.

1389 Cuvier G. 1823. *Recherches sur les ossemens fossils*. Paris: Chez Deterville.

1390 Deméré TA, Berta A, McGowen MR. 2005. The taxonomic and evolutionary history of fossil and
1391   modern balaenopteroid mysticetes. *Journal of Mammalian Evolution* 12:99–143.

1392 De Schepper S, Head MJ, Louwye S (2009). Pliocene dinoflagellate cyst stratigraphy,
1393   palaeoecology and sequence stratigraphy of the Tunnel-Canal Dock, Belgium. *Geological*
1394   *magazine* 146:92–112.

1395 Desmoulins A. 1822. Baleine. *Dictionnaire Classique d'Histoire Naturelle*. Paris: Baudouin
1396 Frères.

1397 Ehret DJ, Macfadden BJ, Jones DS, Devries TJ, Foster DA, Salas-Gismondi R. 2012. Origin of
1398   the white shark *Carcharodon* (Lamniformes: Lamnidae) based on recalibration of the
1399   Upper Neogene Pisco Formation of Peru. *Palaeontology* 55:1139-1153.

1400 El Adli JJ, Deméré TA, Boessenecker RW. 2014. *Herpetocetus morrowi* (Cetacea: Mysticeti), a

1401   new species of diminutive baleen whale from the Upper Pliocene (Piacenzian) of

1402   California, USA, with observations on the evolution and relationships of the Cetotheriidae.

1403   *Zoological Journal of the Linnean Society* 170:400–466.

1404 Evans AR, Jones D, Boyer AG, Brown JH, Costa DP, Morgan ESK, Fitzgerald EMG, Fortelius

1405   M, Gittleman JL, Hamilton MJ, Harding ME, Lintulaakso K, Kathleen Lyons S, Okie JG,

1406   Saarinen JJ, Sibly RM, Smith FA, Stephens PR, Theodor JM, Uhen MD. 2012. The

1407   maximum rate of mammal evolution. *PNAS* 109:4187–4190.

1408 Field DJ, Boessenecker R, Racicot RA, Ásbjörnsdóttir L, Jónasson K, Hsiang AY, Behlke AD,

1409   Vinther J. 2017. The oldest marine vertebrate fossil from the volcanic island of Iceland: a

1410   partial right whale skull from the high latitude Pliocene Tjörnes Formation. *Palaeontology*

1411   60:141-148.

1412 Fitch WM. 1971. Toward defining the course of evolution: minimum change for a specific tree

1413   topology. *Systematic Zoology* 20:406–416.

1414 Flower WH. 1864. Notes on the skeletons of whales in the principal museums of Holland and

1415   Belgium, with descriptions of two species apparently new to science. *Proceedings of the*

1416   *Zoological Society of London* 1864:384–420.

1417 Fordyce RE, de Muizon C. 2001. Evolutionary history of cetaceans: a review. Pp. 169–234 in J.-

1418   M. Mazin and V. de Buffrenil (eds.). Secondary adaptation of tetrapods to life in water. Verlag

1419   Dr. Friedrich Pfeil, Munich.

1420 Fortune SME, Trites AW, Perryman WL, Moore MJ, Pettis HM, Lynn MS. 2012. Growth and

1421   rapid early development of North Atlantic right whales (*Eubalaena glacialis*). *Journal of*

1422   *Mammalogy* 93:1342–1354.

1423 Fraser FC, Purves PE. 1960. Hearing in cetaceans. *Bulletin of the British Museum (Natural*

1424 *History), Zoology* 7:1–140.

1425 Gaines CA, Hare MP, Beck SE, Rosenbaum HC (2005) Nuclear markers confirm taxonomic status

1426 and relationships among highly endangered and closely related right whale species.

1427 *Proceedings of the Royal Society of London. Series B, Biological Sciences* 272:533–542.

1428 Gaskin DE. 1986. The ecology of whales and dolphins. London: Heineman.

1429 Geisler, J. & Sanders, A. E. 2003. Morphological evidence for the phylogeny of Cetacea. *Journal*

1430 *of Mammalian Evolution* 10:23–129.

1431 George JC, Stimmelmayr R, Suydam R, Usip S, Givens G, Sformo T, Thewissen JGM. 2016.

1432 Severe bone loss as part of the life history strategy of bowhead whales. *PLOS ONE* 11(6):

1433 e0156753. DOI:10.1371/journal.pone.0156753.

1434 Gol'din P, Startsev D, Krakhmalnaya T. 2014. The anatomy of the Late Miocene baleen whale

1435 *Cetotherium riabinini* from Ukraine. *Acta Palaeontologica Polonica* 59:795–814.

1436 Gol'din P, Steeman ME. 2015. From problem taxa to problem solver: a new Miocene family,

1437 Tranatocetidae, brings perspective on baleen whale evolution. *PLOS ONE* 10(9):e0135500.

1438 DOI:10.1371/journal.pone.0135500.

1439 Goloboff PA, Farris JS, Nixon KC. 2008. TNT, a free program for phylogenetic analysis.

1440 *Cladistics* 24:774–786.

1441 Gray JE. 1864. On the Cetacea which have been observed in the seas surrounding the British

1442 Islands. *Proceedings of the Scientific Meetings of the Zoological Society of London* 1864:195–

1443 248

1444 Gray JE. 1825. Outline of an attempt at the disposition of the Mammalia into tribes and families

1445   with a list of the genera apparently appertaining to each tribe. *Philosophical Annals* 26:337–

1446   344.

1447 Haile-Selassie Y, Melillo SM, Su DF. 2016. The Pliocene hominin diversity conundrum: do more

1448   fossils mean less clarity. *Proceedings of the National Academy of Sciences USA* 113:6364–

1449   6371.

1450 Hall BK. (ed.) 1996. Homology. Wiley, New York, 266 pp.

1451 Hasse G. 1909. Les morses du Pliocène poederlien à Anvers. *Bulletin de la Société Belge de*

1452   *Géologie, de Paléontologie et d'Hydrogéologie* 23:293–322.

1453 Heath T, Shannon A, Hedtke M, Hillis DM. 2008. Taxon sampling and the accuracy of

1454   phylogenetic analyses. *Journal of Systematics and Evolution* 46:239–257.

1455 Heinzelin J de. 1950. Stratigraphie pliocene et quaternaire observée au Kruisschans. I. Analyse

1456   stratigraphique; II. Conclusions. *Bulletin de l'Institut Royal des Sciences Naturelles de*

1457   *Belgique,* 26(40-41):1–60.

1458 Heinzelin J de. 1952. Note sur les coupes de l'écluse Baudouin à Anvers. *Bulletin de la Société*

1459   *Belge de Géologie* 61(1):106–108.

1460 Heinzelin J de. 1955a. Considérations nouvelles sur le Néogène de l'Ouest de l'Europe. *Bulletin de*

1461   *la Société Belge de Géologie* 64:463–476.

1462 Heinzelin J de. 1955b. Deuxième série d'observations stratigraphiques au Kruisschans. Coupes de

1463   l'écluse Baudouin. I. Analyse stratigraphique; II. Conclusions. *Bulletin de l'Institut Royal des*

1464   *Sciences Naturelles de Belgique* 31(66-67):1–43.

1465 Huelsenbeck JP. 1994. Comparing the stratigraphic record to estimates of phylogeny.

1466   *Paleobiology* 20:470–483.

1467 Jackson JA, Baker CS, Vant M, Steel DJ, Medrano-Gonzalez L, Palumbi SR. 2009. Big and slow:

1468   Estimates of molecular evolution in baleen whales (suborder Mysticeti). *Molecular Biology*

1469   *and Evolution* 26:2427–2440.

1470 Kaliszewska ZA, Seger J, Rowntree VJ, Barco SG, Benegas R, Best PB, Brown MW, Brownell

1471   RL Jr, Carribero A, Harcourt R, Knowlton AR, Marshalltilas K, Patenaude NJ, Rivarola M,

1472   Schaeff CM, Sironi M, Smith WA, Yamada TK. 2005. Population histories of right whales

1473   (Cetacea: *Eubalaena*) inferred from mitochondrial sequence diversities and divergences of

1474   their whale lice (Amphipoda: *Cyamus*). *Molecular Ecology* 14:3439–3456.

1475 Keane M, Semeiks J, Webb AE, Li YI, Quesada V, Craig T, Madsen LB, van Dam S, Brawand D,

1476   Marques PI, Michalak P, Kang L, Bhak J, Yim H-S, Grishin NV, Nielsen NH, Heide-

1477   Jørgensen MP, Oziolor EM, Matson CW, Church GM, Stuart GW, Patton JC, George JC,

1478   Suydam R, Larsen K, Lòpez-Otìn C, O'Connell MJ, Bickham JW, Thomsen B, de Magalhães

1479   JP. 2015. Insights into the Evolution of Longevity from the Bowhead Whale Genome. *Cell*

1480   *Reports* 10:112–122.

1481 Kellogg R. 1928. The history of whales – their adaptation to life in the water. *Quarterly Review of*

1482   *Biology* 3:29–76; and 174–208.

1483 Kenney RD. 2009. North Atlantic, North Pacific, and Southern right whales. In: Perrin WF,

1484   Wursig B, Thewissen JGM, eds. *Encyclopedia of Marine Mammals*. San Diego: Academic

1485   Press, 806–813.

1486 Kimura T. 2009. Review of fossil balaenids from Japan with a re-description of *Eubalaena*

1487   *shinshuensis* (Mammalia, Cetacea, Mysticeti). *Quaderni del Museo di Storia Naturale di*

1488   *Livorno* 22:3–21.

1489   Koshi WR, Davis RA, Miller GW, Withrow DE. 1993. Reproduction. In: Burns JJ, Montague JJ,

1490   Cowles CJ, eds. *The bowhead whale. The Society for Marine Mammalogy Special Publication*

1491   2:239–274.

1492   Laga P, Louwye S, Mostaert F. 2006. Disused Neogene and Quaternary regional stages from

1493   Belgium: Bolderian, Houthalenian, Antwerpian, Diestian, Deurnian, Kasterlian,

1494   Kattendijkian, Scaldisian, Poederlian, Merksemian and Flandrian. *Geologica Belgica,* 9:215–

1495   224.

1496   Lambert O. 2008. A new porpoise (Cetacea, Odontoceti, Phocoenidae) from the Pliocene of the

1497   North Sea. *Journal of Vertebrate Paleontology* 28:863–872.

1498   Linnaeus C. 1758. *Systema Naturae*. Stockholm: Salvii.

1499   Louwye S, Head MJ, De Schepper S. 2004. Dinoflagellate cyst stratigraphy and palaeoecology of

1500   the Pliocene in northern Belgium, southern North Sea Basin. *Geological Magazine* 141:353-

1501   378.

1502   Maddison DR, Maddison WP. 2000. *MacClade 4: Analysis of phylogeny and character evolution.*

1503   *Version 4.0*. Sunderland: Sinauer Associates.

1504   Malik, S., Brown, M.W., Kraus, S.D. & B.N. White, 2000. Analysis of mitochondrial DNA

1505   diversity within and between North and South Atlantic right whales. *Marine Mammal Science*

1506   16:545–559.

1507   Manganelli G, Benocci A. 2014. I cetacei fossili del Museo dell'Accademia dei Fisiocritici di

1508   Siena. *Museologia Scientifica Memorie* 13:103–110.

1509   Marquet R. 1993. The molluscan fauna of the Kruisschans Member (Lillo Formation, Late

1510   Pliocene) in the Antwerp area (Belgium). *Contributions to Tertiary and Quaternary Geology*

1511   30:83–103.

1512 Marx FG. 2011. The more the merrier? A large cladistics analysis of mysticetes, and comments on

1513   the transition from teeth to baleen. *Journal of Mammalian Evolution* 18:77–100.

1514 Marx FG, Fordyce RE 2015. Baleen boom and bust: a synthesis of mysticete phylogeny, diversity

1515   and disparity. *Royal Society Open Science* 2:140434.

1516 Marx FG, Fordyce RE. 2016. A link no longer missing: new evidence for the cetotheriid affinities

1517   of *Caperea*. *PLOS ONE* 11(10):e0164059. DOI:10.1371/journal.pone.0164059.

1518 McLeod SA, Whitmore FC Jr, Barnes LG. 1993. Evolutionary relationships and classification. In:

1519   Burns JJ, Montague JJ, Cowles CJ eds. *The Bowhead whale*. *The Society for Marine*

1520   *Mammalogy, Special Publication* 2:45–70.

1521 Mead JG, Fordyce RE. 2010. The therian skull. A lexicon with emphasis on the odontocetes.

1522   *Smithsonian Contributions to Zoology* 627:1–248.

1523 Miller GS. 1923. The telescoping of the cetacean skull. *Smithsonian Miscellaneous Collections*

1524   76:1–70.

1525 Misonne X. 1958. Faune du Tertiaire et du Pléistocène inférieur de Belgique (Oiseaux et

1526   Mammifères). *Bulletin de l'Institut Royal des Sciences Naturelles de Belgique* 34(5):1–36.

1527 Mitchell ED. 1989. A new cetacean from the late Eocene La Meseta Formation, Seymour Island,

1528   Antarctic Peninsula. *Canadian Journal of Fisheries and Aquatic Sciences* 46:2219–2235.

1529 Moran MM, Bajpai S, George JC, Suydam R, Usip S, Thewissen JGM. 2014. Intervertebral and

1530   epiphyseal fusion in the postnatal ontogeny of cetaceans and terrestrial mammals. *Journal*

1531   *of Mammalian Evolution* 22:93–109.

1532 Morgan GS. 1994. Miocene and Pliocene marine mammal faunas from the Bone Valley Formation

1533   of Central Florida. *Proceedings of the San Diego Society of Natural History* 29:239-268.

1534   Nishiwaki M, Hasegawa Y. 1969. The discovery of the right whale skull in the Kisagata shell bed.

1535   *The Scientific Reports of the Whale Research Institute Tokyo* 21:79–84.

1536   Omura H. 1958. North Pacific right whale. *The Scientific Reports of the Whale Research Institute*

1537   *Tokyo* 13:1– 52.

1538   Pastene LA, Goto M, Kanda N, Zerbini AN, Kerem D, Watanabe K, Bessho Y, Hasegawa M,

1539   Nielsen R, Larsen F, Palsbøll PJ. 2007. Radiation and speciation of pelagic organisms during

1540   periods of global warming: the case of the common minke whale, *Balaenoptera acutorostrata*.

1541   *Molecular Ecology* 16:1481–1495.

1542   Paul CRC. 1992. The recognition of ancestors. *Historical Biology* 6:239–250.

1543   Pivorunas A. 1979. The fibrocartilage skeleton and related structures of the ventral pouch of

1544   balaenopterid whales. *Journal of Morphology* 151:299–314.

1545   Plisnier-Ladame F, Quinet GE. 1969. *Balaena belgica* Abel 1938 Cetace du Merxemien d'Anvers.

1546   *Bulletin de l'Institut Royal des Sciences Naturelles de Belgique* 45(3):1–6.

1547   Pyenson ND, Sponberg SN. 2011. Reconstructing body size in extinct crown Cetacea (Neoceti)

1548   using allometry, phylogenetic methods, and tests from the fossil record. *Journal of*

1549   *Mammalian Evolution* 18:269–289.

1550   Quental TA, Marshall CR. 2010. Diversity dynamics: molecular phylogenies need the fossil

1551   record. *Trends in Ecology and Evolution* 25:434–441.

1552   Rice DW. 2009. Classification. In Perrin WF, Wursig B, Thewissen JGM eds. *Encyclopedia of*

1553   *Marine Mammals*. San Diego: Academic Press, 231–234.

1554   Rooney AP, Honeycutt RL, Derr JN. 2001. Population size change of Bowhead whales inferred

1555   from DNA sequence polymorphism data. *Evolution* 55:1678–1685.

1556 Rosenbaum HC, Brownell RL Jr, Brown MW, Schaeff C, Portway V, White BN, Malik S, Pastene

1557   LA, Patenaude NJ, Baker CS, Goto M, Best PB, Clapham PJ, Hamilton P, Moore M, Payne

1558   R, Rowntree V, Tynan CT, Bannister JL, Salle RD. 2000. World-wide genetic differentiation

1559   of *Eubalaena*: questioning the number of right whale species. *Molecular Ecology* 9:1793–

1560   1802.

1561 Sanderson LR, Wassersug R. 1993. Convergent and alternative designs for vertebrate suspension

1562   feeding. In: Hanken J, Hall BK eds. *The skull*. Vol. 3. Chicago: University Press of Chicago,

1563   37–112.

1564 Santangelo G, Bisconti M, Santini F, Bramanti L 2005. Estinzioni e conservazione: il ruolo dei

1565   modelli nello studio e nella tutela della diversità biologica. *Biology Forum* 98:13–18.

1566 Sarti C, Lanzetti A. 2014. I cetacei fossili del Museo Geologico Giovanni Capellini dell'Università

1567   di Bologna. *Museologia Scientifica Memorie* 13:70–78.

1568 Sasaki T, Nikaido M, Hamilton H, Goto M, Kato H, Kanda N, Pastene LA, Cao Y, Fordyce RE,

1569   Hasegawa M, Okada N. 2005. Mitochondrial phylogenetics and evolution of mysticete

1570   whales. *Systematic Biology* 54:77–90.

1571 Scannella JB, Fowler DW, Goodwin MB, Horner JR. 2014. Evolutionary trends in *Triceratops*

1572   from the Hell Creek Formation, Montana. *Proceedings of the National Academy of Sciences*

1573   *USA* 111:10245–10250.

1574 Seehausen O. 2006. African cichlid fish: a model system in adaptive radiation research.

1575   *Proceedings of the Royal Society B* 273: DOI: 10.1098/rspb.2006.3539.

1576 Shaller O. 1999. *Nomenclatura anatomica veterinaria illustrate*. Roma: Antonio Delfino Editore.

1577 Silva M, Downing JA. 1995. The allometric scaling of density and body mass: a nonlinear

1578   relationship for terrestrial mammals. *The American Naturalist* 145:704–727.

1579   Steeman ME, Hebsgaard MB, Fordyce RE, Ho SYW, Rabosky DL, Nielsen R, Rahbek C, Glenner

1580   H, Sørensen MV, Willerslev E. 2009. Radiation of extant cetaceans driven by restructuring of

1581   the oceans. *Systematic Biology* 58:573–585.

1582   Tomilin AG. 1967. Cetacea. In: Heptner VG ed. *Mammals of the USSR and adjacent countries*.

1583   Vol. 9. Jerusalem: Israel Program for Scientific Translations, 1–717.

1584   Trites AD, Pauly D. 1998. Estimating mean body masses of marine mammals from maximum

1585   body lengths. *Canadian Journal of Zoology* 76:886–896.

1586   True FW. 1904. The whalebone whales of the western north Atlantic, compared with those

1587   occurring in European waters; with some observations on the species of the north Pacific.

1588   *Smithsonian Contributions to Knowledge* 33:1–332.

1589   Tsai C-H, Fordyce RE. 2015. Ancestor-descendant relationships in evolution: origin of the extant

1590   pygmy right whale, *Caperea marginata*. *Biology Letters* 11:20140875. DOI:

1591   http://dx.doi.org/10.1098/rsbl.2014.0875.

1592   Uhen MD. 2008. New protocetid whales from Alabama and Mississippi, and a new cetacean clade,

1593   Pelagiceti. *Journal of Vertebrate Paleontology* 28:589–593.

1594   Uhen MD, Gingerich PD. 2001. New genus of dorudontine archaeocete (Cetacea) from the

1595   middle-to-late Eocene of South Carolina. *Marine Mammal Science* 17:1–34.

1596   Vandenberghe N, Laga P, Steurbaut E, Hardenbol J, Vail PR. 1998. Tertiary sequence stratigraphy

1597   at the southern border of the North Sea Basin in Belgium. *Special Publication-SEPM,* 60:119–

1598   154.

1599   Wagner PJ. 2000. Exhaustion of morphologic character states among fossil taxa. *Evolution*

1600   54:365–386.

1601 Yamada TK, Chou L-S, Chantrapornsyl S, Adulyanukosol K, Chakravarti SK, Oishi M, Wada S,

1602 Yao C-J, Kakuda T, Tajima Y, Arai K, Umetani A, Kurihara N. (2006). Middle sized

1603 balaenopterid whale specimens (Cetacea: Balaenopteridae) preserved at several institutions in

1604 Taiwan, Thailand, and India. *Memoirs of the National Science Museum, Tokyo* 44:1–10.

1605 Zachos J, Pagani M, Sloan L, Thomas E, Billups K. 2001. Trends, rhythms, and aberrations in

1606 global climate 65 Ma to present. *Science* 292:686–693.

1607

1608

1609

1610

1611

1612 **CAPTIONS TO TEXT-FIGURES AND TABLES**

1613

1614 **Figure 1**

1615 Localities of the balaenids described in this paper. A, Localization of Antwerp in Belgium and its

1616 relationships with the North Sea. Grey whading represents marine Pliocene deposits. B, Detailed

1617 map of the Antwerp harbor showing the first Kruisschans lock, where the holotype of *Eubalaena*

1618 *ianitrix* sp. nov. (RBINS M. 879a-f) and the fragment of maxilla RBINS M. 880 were found. The

1619 cervical vertebrae RBINS M. 881 were discovered in the "Darses I-II" in Oorderen. Modified from

1620 De Schepper et al., 2009.

1621

1622 **Figure 2**

1623 Lithological units from the Pliocene of the Antwerp area. Formations, members and their ages are

1624 provided, including the Kruisschans Sands Member of the Lillo Formation in the Piacenzian (Late

1625 Pliocene), where the neurocranium RBINS M. 879, holotype of *Eubalaena ianitrix* sp. nov., was

1626 discovered. Positions along the local lithostratigraphic column of other balaenid specimens from

1627 the Antwerp area investigated in this work are also provided: right maxilla RBINS M. 880,

1628 Balaenidae gen. et sp. indet.; cervical complex RBINS M. 881, Balaenidae gen. et sp. indet.; left

1629 humerus RBINS M. 2280, *Eubalaena* sp. Modified from De Schepper et al., 2009.

1630

1631 **Figure 3**

1632 The cervical vertebrae RBINS M. 881 representing the cotype of *'Balaena' belgica* by Abel (1941)

1633 and reassigned to Balaenidae gen. et sp. indet. in this work. A, anterior view. B, left lateral view.

1634 C, posterior view. D, right lateral view. E, ventral view. F, dorsal view. Scale bar equals 10 cm.

1635

1636

1637

1638 **Figure 4**

1639 The fragment of right maxilla RBINS M. 880 assigned to Balaenidae gen. et sp. indet. in this work.

1640 A, dorsolateral view. B, dorsomedial view. C, ventromedial view. Scale bar equals 30 cm.

1641

1642 **Figure 5**

1643 The left humerus RBINS M. 2280 assigned to *Eubalaena* sp. in this work. A, lateral view. B,

1644 anterior view. C, distal view of articular facets for radius and ulna. D, proximal view or articular

1645 head for scapula. E, posterior view. F, medial view. Scale bars equal 10 cm.

1646

1647 **Figure 6**

1648 *Eubalaena ianitrix* sp. nov. (holotype RBINS M. 879). Dorsal view of neurocranium. A,

1649 photographic representation. B, interpretation. Scale bar equals 50 cm. Anatomical abbreviations:

1650 fm, foramen magnum; fr, frontal; irfr, interorbital region of the frontal; oc, occipital condyles; smc,

1651 supramastoid crest; sq, squamosal; sop, supraorbital process of the frontal.

1652

1653 **Figure 7**

1654 *Eubalaena ianitrix* sp. nov. (holotype RBINS M. 879). Left lateral view of neurocranium. A,

1655 photographic representation. B, interpretation. Scale bar equals 50 cm. Anatomical abbreviations:

1656 fm, foramen magnum; fr, frontal; irfr, interorbital region of the frontal; oc, occipital condyle; orb,

1657 orbit; otc, orbitotemporal crest; par, parietal; pgl, postglenoid process of squamosal; p-fr, parietal-

1658 frontal suture; p-sq, parietal-squamosal suture; smc, supramastoid crest; soc, supraoccipital; sop,

1659 supraorbital process of frontal; sq, squamosal; vom, vomer; zyg, zygomatic process of squamosal;

1660 *, anterolateral corner of parietal-frontal suture.

1661

1662

1663

1664 **Figure 8**

1665 *Eubalaena ianitrix* sp. nov. (holotype RBINS M. 879). Right lateral view of neurocranium. A,

1666 photographic representation. B, interpretation. Scale bar equals 50 cm. Anatomical abbreviations:

1667 fm, foramen magnum; fr, frontal; irfr, interorbital region of the frontal; oc, occipital condyle; orb,

1668 orbit; otc, orbitotemporal crest; par, parietal; pgl, postglenoid process of squamosal; p-fr, parietal-

1669 frontal suture; p-sq, parietal-squamosal suture; smc, supramastoid crest; soc, supraoccipital; sop,

1670 supraorbital process of frontal; sq, squamosal; vom, vomer; zyg, zygomatic process of squamosal;

1671 *, anterolateral corner of parietal-frontal suture.

1672

1673 **Figure 9**

1674 *Eubalaena ianitrix* sp. nov. (holotype RBINS M. 879). Anterior view of neurocranium. A,

1675 photographic representation. B, interpretation. Scale bar equals 50 cm. Anatomical abbreviations:

1676 fr, frontal; irfr, interorbital region of the frontal; max-fr, grooves for articulation of maxilla and

1677 frontal; mes, mesethmoid; nas-fr, groove for articulation of nasal and frontal; pal, palatine; par,

1678 parietal; pgl, postglenoid process of squamosal; pm-fr, grooves for articulation of premaxilla and

1679 frontal; soc, supraoccipital; sop, supraorbital process of frontal; sq, squamosal; vom, vomer; zyg,

1680 zygomatic process of squamosal.

1681

1682   **Figure 10.**

1683   *Eubalaena ianitrix* sp. nov. (holotype RBINS M. 879). Ventral view of neurocranium. A,

1684   photographic representation. B, interpretation. Scale bar equals 50 cm. Anatomical abbreviations:

1685   exo, exoccipital; fm, foramen magnum; fr, frontal; sop, supraorbital process of frontal; oc, occipital

1686   condyle; och, optic channel; or, orbit; pgl, postglenoid process of squamosal; pt, pterygoid; sq,

1687   squamosal; vom, vomer; zyg, zygomatic process of squamosal.

1688

1689

1690   **Figure 11**

1691   *Eubalaena ianitrix* sp. nov. (holotype RBINS M. 879). Posterior view of neurocranium. A,

1692   photographic representation. B, interpretation. Scale bar equals 50 cm. Anatomical abbreviations:

1693   boc, basioccipital; bop, basioccipital protuberance; exo, exoccipital; fm, foramen magnum; fr,

1694   frontal; jn, jugular notch; oc, occipital condyle; pal, palatine; pgl, postglenoid process of

1695   squamosal; pt, pterygoid; ptf, pterygoid fossa; sop, supraorbital process of frontal; sq, squamosal;

1696   vom, vomer; zyg, zygomatic process of squamosal.

1697

1698   **Figure 12**

1699   Phylogenetic relationships of Mysticeti with focus on Balaenoidea. Single most-parsimonious

1700   cladogram with the following tree statistics: Consistency Index (CI), 0.508; Retention Index (RI),

1701   0.805; Rescaled CI, 0.40894; Homoplasy Index (HI), 0.492; Stratigraphic Consistency Index

1702   (SCI), 0.825.

1703

1704 **Figure 13**

1705 Schematic representation of diagnostic characters observed in the holotype skull of *Eubalaena*

1706 *ianitrix* in left lateral view. Not to scale.

1707

1708 **Figure 14**

1709 Phylogenetic relationships of Balaenidae plotted against a time scale in million years (Ma). Bold

1710 lines represent stratigraphic ages of taxa based on dated specimens; light lines represent inferred

1711 presence of taxa. Note that three time periods are highlighted: (1) separation of Balaenidae and

1712 Neobalaenidae inferred to have occurred *c.* 11 Ma (latest Serravallian-to-earliest Tortonian); (2)

1713 separation of the *Balaena + Balaenella* clade and the *Eubalaena + Balaenula* clade inferred to

1714 have occurred *c.* 7 Ma (latest Tortonian-to-earliest Messinian); and (3) origin of the extant

1715 *Eubalaena* species inferred to have occurred *c.* 2.5 Ma (latest Zanclean-to-earliest Piacenzian).

1716

1717

1718 **Table 1**

1719 Measurements (in mm) of RBINS M. 880 (cervical vertebrae complex, Balaenidae gen. et sp.

1720 indet.) and M. 2280 (left humerus, *Eubalaena* sp.). Characters are measured as preserved.

1721

1722 **Table 2**

1723 Measurements (in mm) of the neurocranium RBINS M. 879a-f (holotype of *Eubalaena ianitrix*

1724 sp. nov.). Characters are measured as preserved.

1725

Figure 1

Fig. 1 - Localities of the balaenids described in this paper.

A, Localization of Antwerp in Belgium and its relationships with the North Sea. Grey whading represents marine Pliocene deposits. B, Detailed map of the Antwerp harbor showing the first Kruisschans lock, where the holotype of *Eubalaena ianitrix* sp. nov. (RBINS M. 879a-f) and the fragment of maxilla RBINS M. 880 were found. The cervical vertebrae RBINS M. 881 were discovered in the "Darses I-II" in Oorderen. Modified from De Schepper et al., 2009.
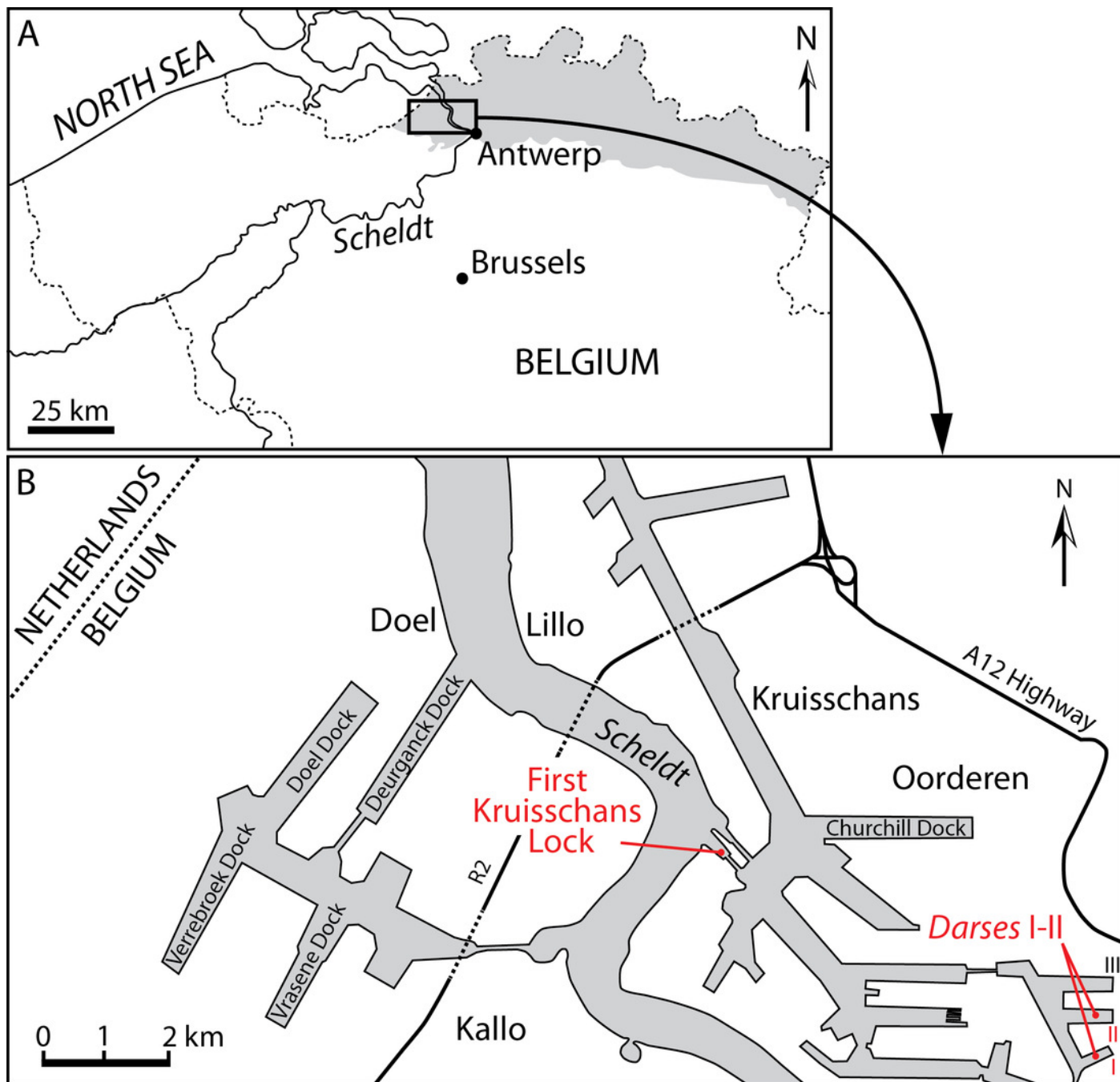
Figure 2

Fig. 2 - Lithological units from the Pliocene of the Antwerp area.

Formations, members and their ages are provided, including the Kruisschans Sands Member of the Lillo Formation in the Piacenzian (Late Pliocene), where the holotype of *Eubalaena ianitrix* sp. nov. was discovered. Modified from De Schepper et al., 2009.
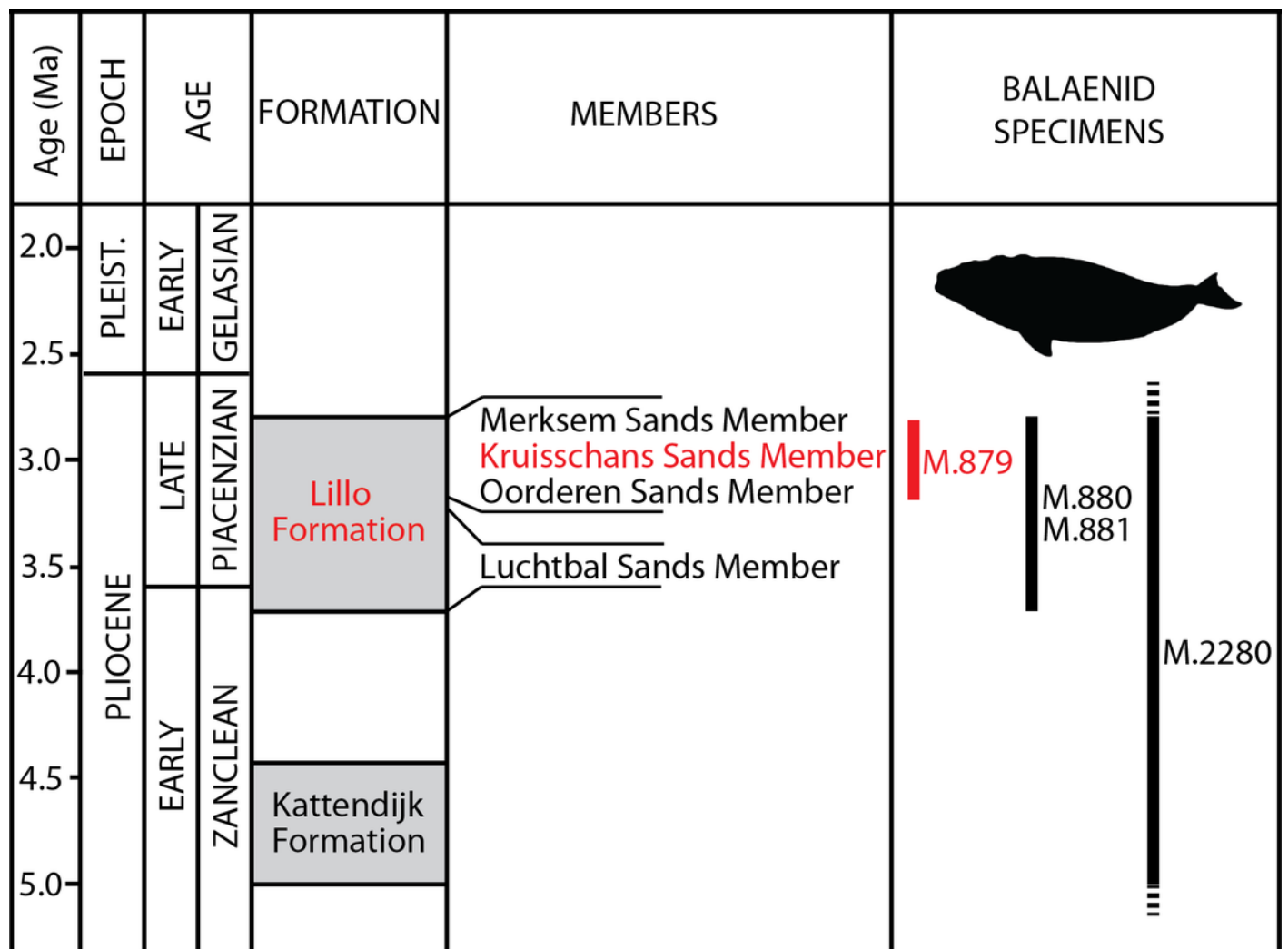
Figure 3

Fig. 3 - The cervical vertebrae RBINS M. 881 that were originally used as type of *'Balaena' belgica* by Abel (1941) and reassigned to Balaenidae gen. et sp. indet. in this work.

A, anterior view. B, left lateral view. C, posterior view. D, right lateral view. E, ventral view. F, dorsal view. Scale bar equals 10 cm.

Figure 4

Fig. 4 - The fragment of right maxilla RBINS M. 880 assigned to Balaenidae gen. et sp. indet. in this work.

A, dorsolateral view. B, dorsomedial view. C, ventromedial view. Scale bar equals 30 cm.

Figure 5

Fig. 5 - The left humerus RBINS M. 2280 assigned to *Eubalaena* sp. in this work.

A, lateral view. B, anterior view. C, distal view of articular facets for radius and ulna. D, proximal view or articular head for scapula. E, posterior view. F, medial view. Scale bars equal 10 cm.
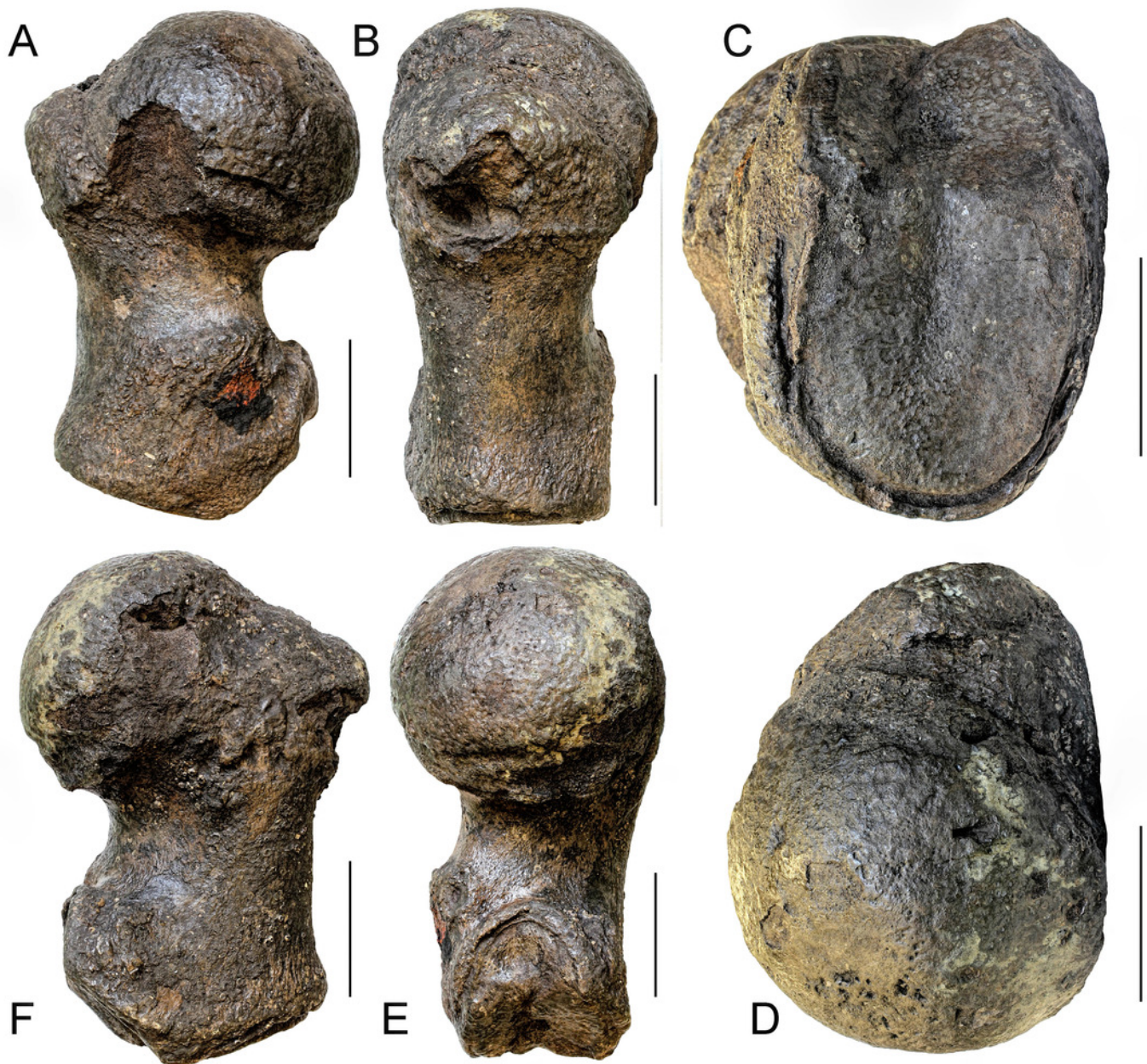
Figure 6

Fig. 6 - *Eubalaena ianitrix* sp. nov. (holotype RBINS M. 879). Dorsal view of neurocranium.

A, photographic representation. B, interpretation. Scale bar equals 50 cm. Anatomical abbreviations: fm, foramen magnum; fr, frontal; irfr, interorbital region of the frontal; oc, occipital condyles; smc, supramastoid crest; sq, squamosal; sop, supraorbital process of the frontal.
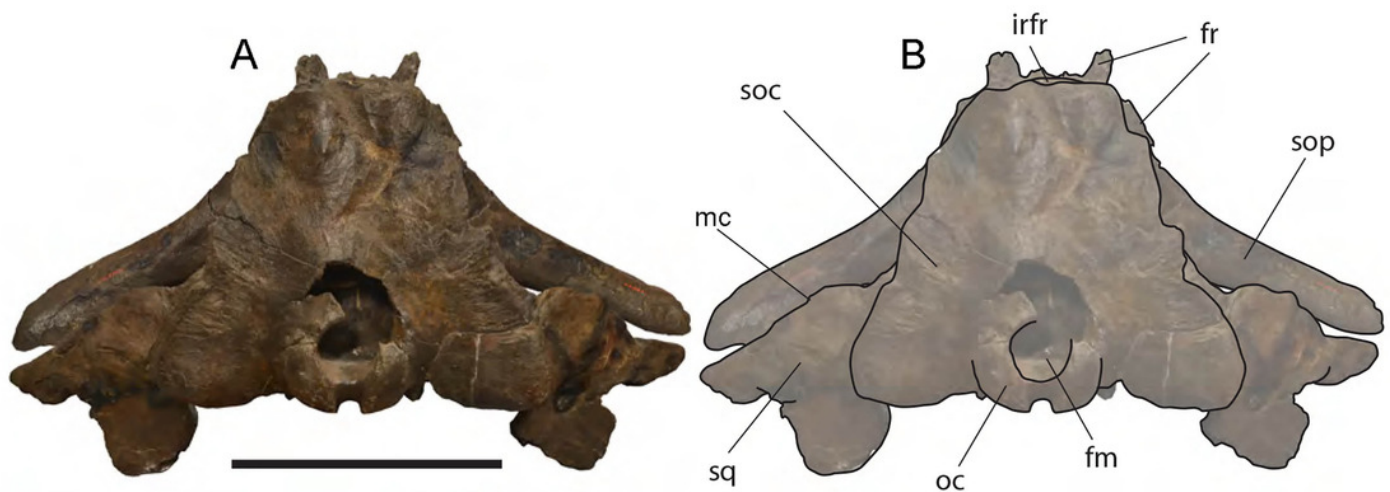
Figure 7

Fig. 7 - *Eubalaena ianitrix* sp. nov. (holotype RBINS M. 879). Left lateral view of neurocranium.

A, photographic representation. B, interpretation. Scale bar equals 50 cm. Anatomical abbreviations: fm, foramen magnum; fr, frontal; irfr, interorbital region of the frontal; oc, occipital condyle; orb, orbit; otc, orbitotemporal crest; par, parietal; pgl, postglenoid process of squamosal; p-fr, parietal-frontal suture; p-sq, parietal-squamosal suture; smc, supramastoid crest; soc, supraoccipital; sop, supraorbital process of frontal; sq, squamosal; vom, vomer; zyg, zygomatic process of squamosal; *, anterolateral corner of parietal-frontal suture.
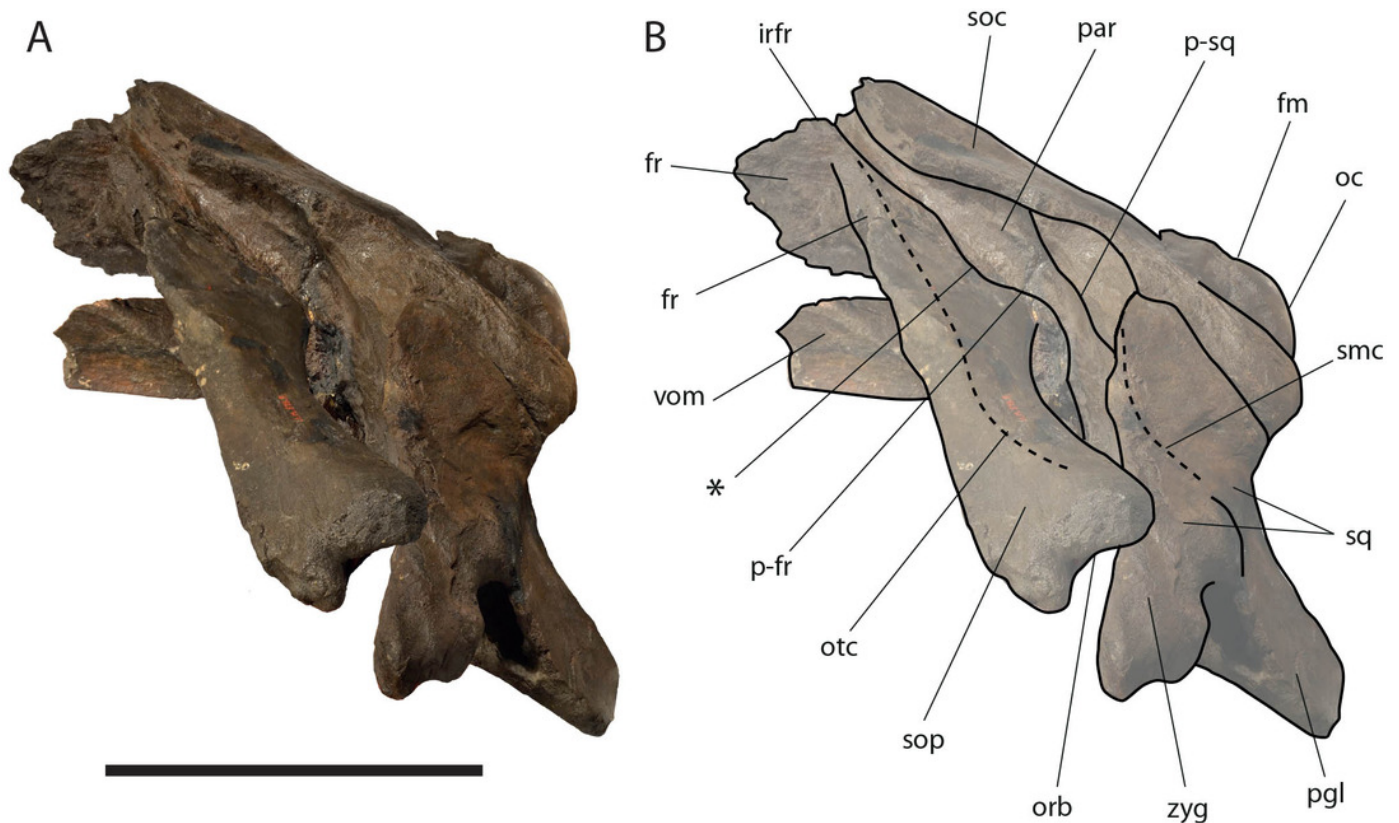
Figure 8

Fig. 8 - *Eubalaena ianitrix* sp. nov. (holotype RBINS M. 879). Right lateral view of neurocranium.

A, photographic representation. B, interpretation. Scale bar equals 50 cm. Anatomical abbreviations: fm, foramen magnum; fr, frontal; irfr, interorbital region of the frontal; oc, occipital condyle; orb, orbit; otc, orbitotemporal crest; par, parietal; pgl, postglenoid process of squamosal; p-fr, parietal-frontal suture; p-sq, parietal-squamosal suture; smc, supramastoid crest; soc, supraoccipital; sop, supraorbital process of frontal; sq, squamosal; vom, vomer; zyg, zygomatic process of squamosal; *, anterolateral corner of parietal-frontal suture.
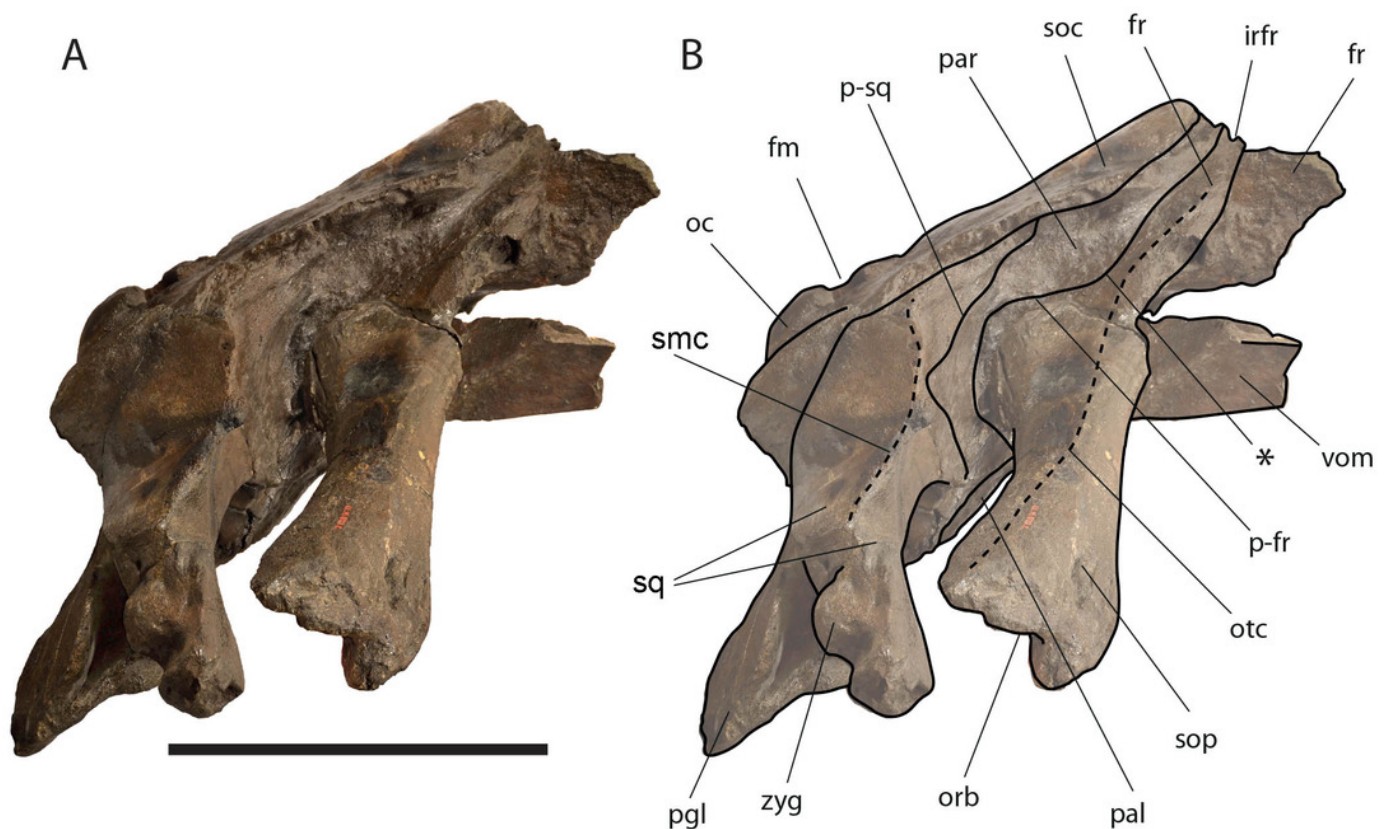
Figure 9

Fig. 9 - *Eubalaena ianitrix* sp. nov. (holotype RBINS M. 879). Anterior view of neurocranium.

A, photographic representation. B, interpretation. Scale bar equals 50 cm. Anatomical abbreviations: fr, frontal; irfr, interorbital region of the frontal; max-fr, grooves for articulation of maxilla and frontal; mes, mesethmoid; nas-fr, groove for articulation of nasal and frontal; pal, palatine; par, parietal; pgl, postglenoid process of squamosal; pm-fr, grooves for articulation of premaxilla and frontal; soc, supraoccipital; sop, supraorbital process of frontal; sq, squamosal; vom, vomer; zyg, zygomatic process of squamosal.
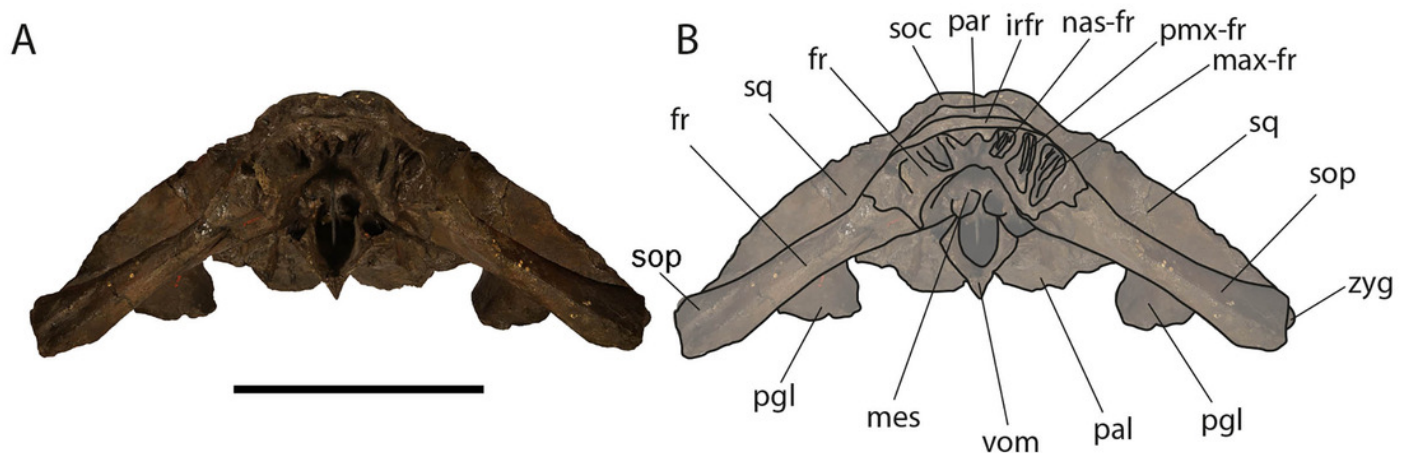
Figure 10

Fig. 10 - *Eubalaena ianitrix* sp. nov. (holotype RBINS M. 879). Ventral view of neurocranium.

A, photographic representation. B, interpretation. Scale bar equals 50 cm. Anatomical abbreviations: exo, exoccipital; fm, foramen magnum; fr, frontal; sop, supraorbital process of frontal; oc, occipital condyle; och, optic channel; or, orbit; pgl, postglenoid process of squamosal; pt, pterygoid; sq, squamosal; vom, vomer; zyg, zygomatic process of squamosal.
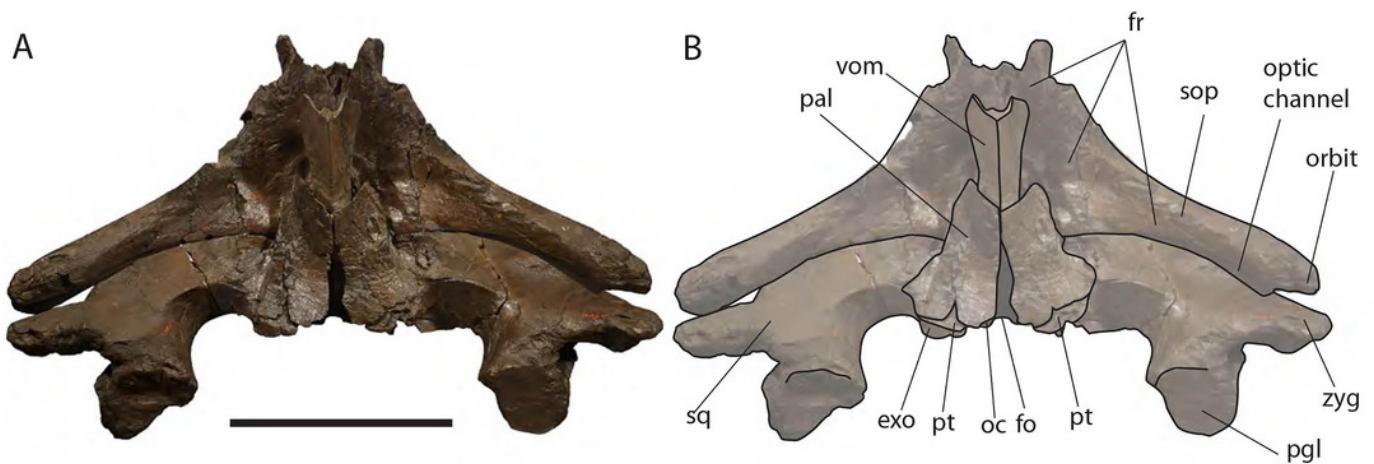
Figure 11

Fig. 11 - *Eubalaena ianitrix* sp. nov. (holotype RBINS M. 879). Posterior view of neurocranium.

A, photographic representation. B, interpretation. Scale bar equals 50 cm. Anatomical abbreviations: boc, basioccipital; bop, basioccipital protuberance; exo, exoccipital; fm, foramen magnum; fr, frontal; jn, jugular notch; oc, occipital condyle; pal, palatine; pgl, postglenoid process of squamosal; pt, pterygoid; ptf, pterygoid fossa; sop, supraorbital process of frontal; sq, squamosal; vom, vomer; zyg, zygomatic process of squamosal.
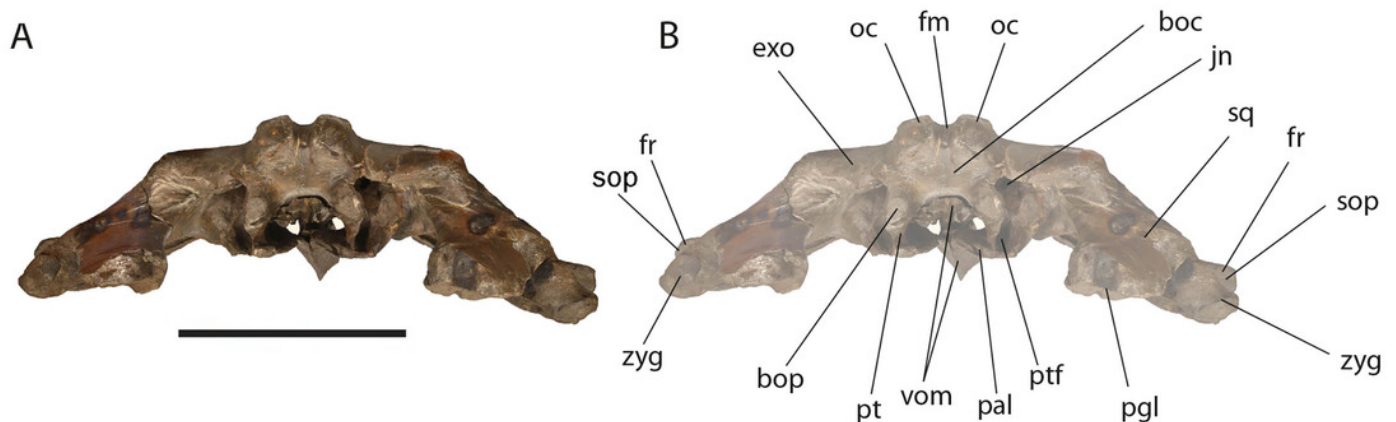
Figure 12

Fig. 12 - Phylogenetic relationships of Mysticeti with focus on Balaenoidea.

Single most-parsimonious cladogram with the following tree statistics: Consistency Index (CI), 0.508; Retention Index (RI), 0.805; Rescaled CI, 0.40894; Homoplasy Index (HI), 0.492; Stratigraphic Consistency Index (SCI), 0.825.
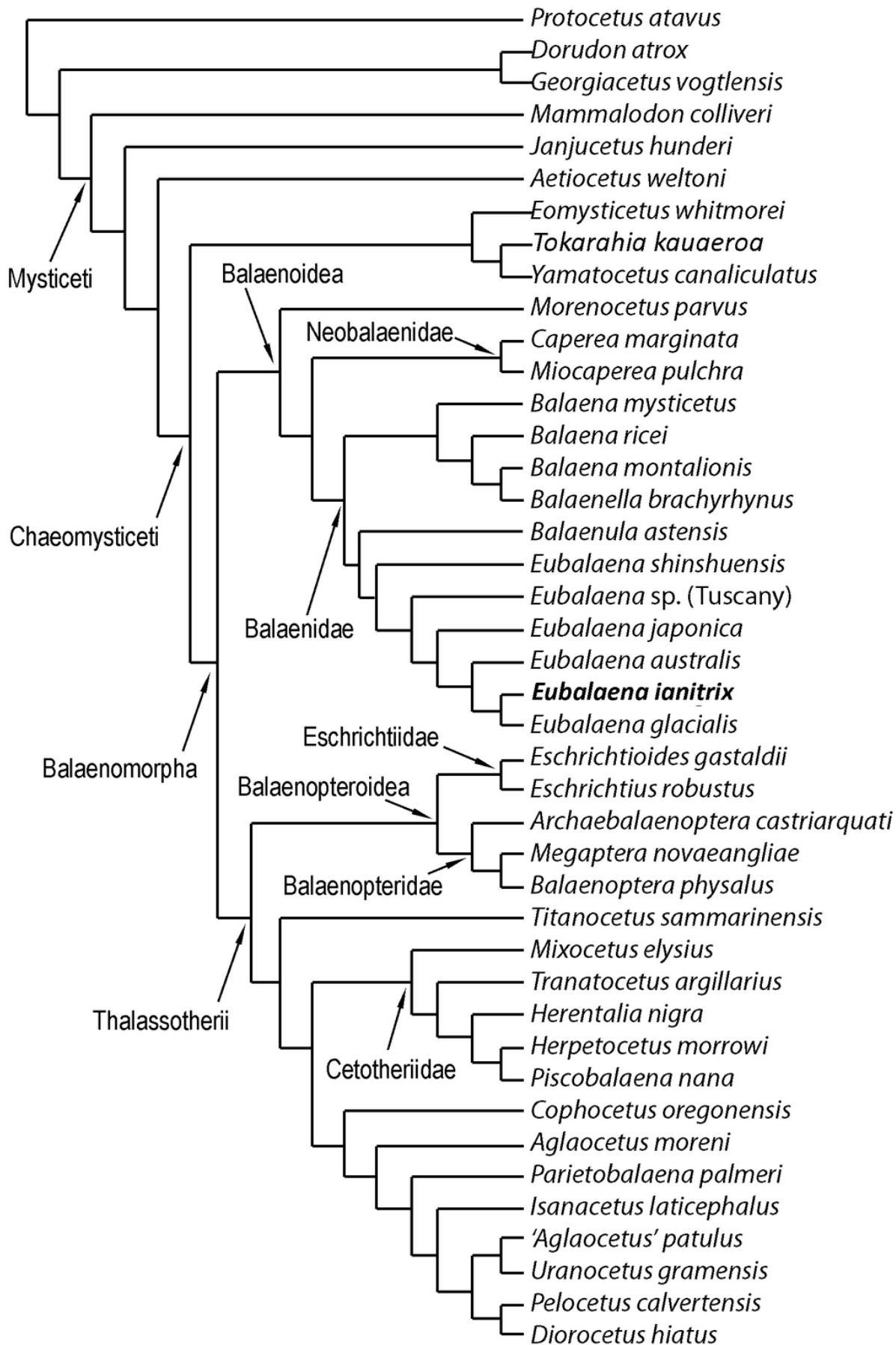
Figure 13

Fig. 13 - Schematic representation of diagnostic characters observed in the holotype skull of *Eubalaena ianitrix* in left lateral view.

Not to scale.
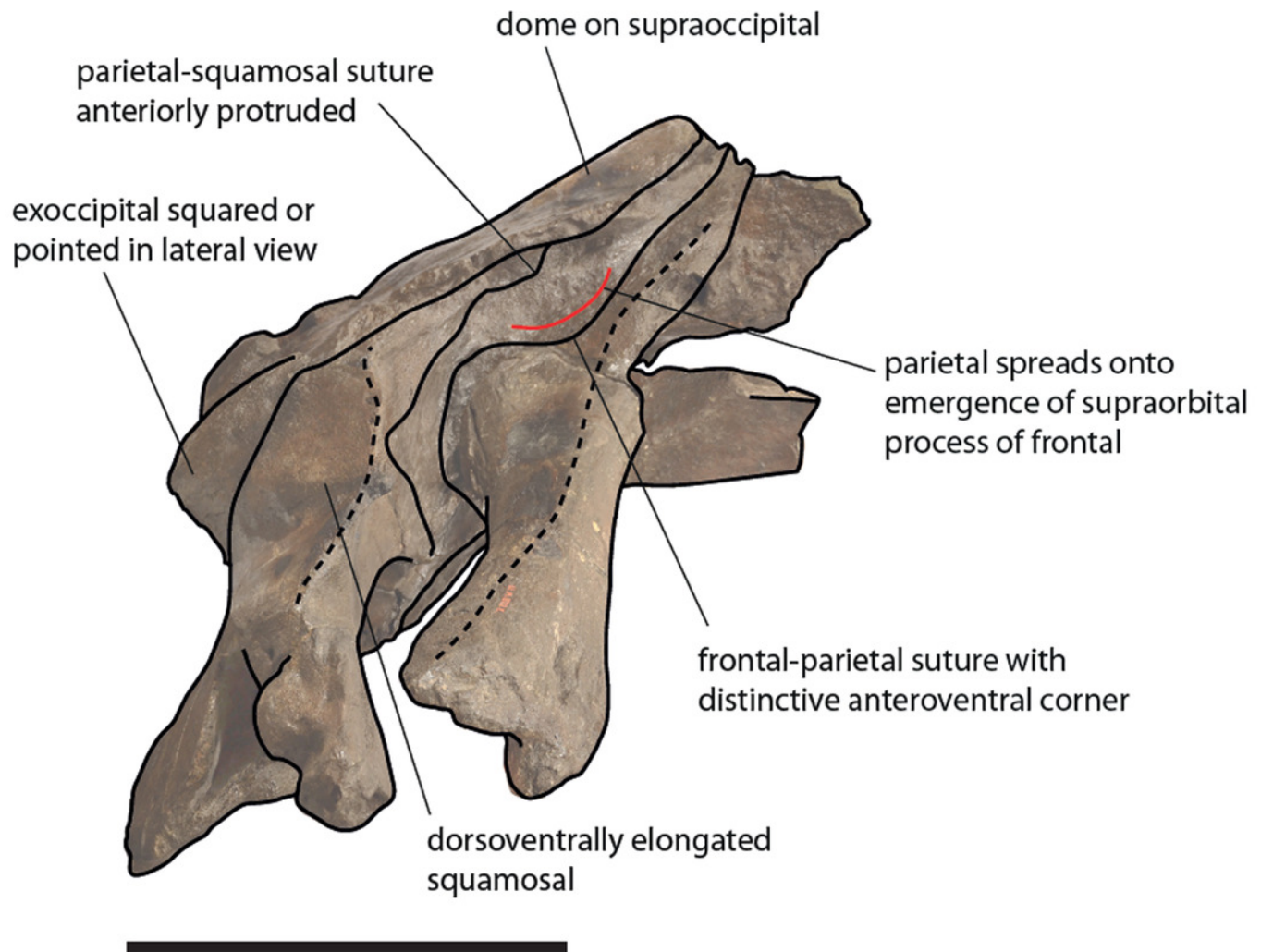
Figure 14

Phylogenetic relationships of Balaenidae plotted against temporal scale

Fig 14 - Phylogenetic relationships of Balaenidae plotted against a temporal scale showing that the separation of Balaenidae and Neobalaenidae occurred before Tortonian at least and that the separation of the *Balaena + Balaenella* clade from the *Eubalaena + Balaenula* clade occurred at the beginning or during the Messinian (latest Miocene). The origin of the modern *Eubalaena* (right whale) is inferred to be occurred at the beginning of the Piacenzian.
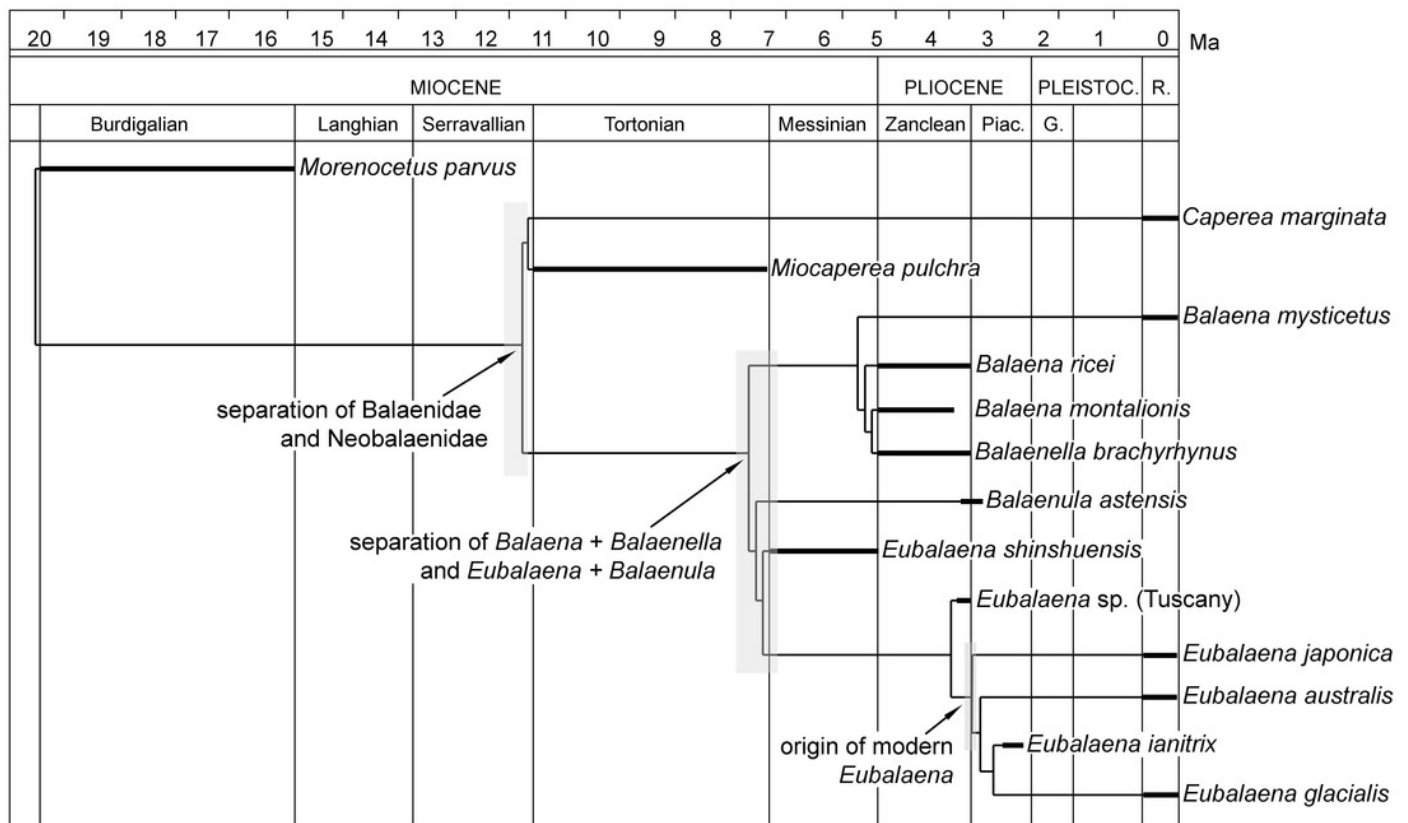
Table 1 - Measurements (in mm) of RBINS M. 880 (cervical vertebrae complex, Balaenidae gen. et sp. indet.) and M. 2280 (left humerus, *Eubalaena* sp.).

Characters are measured as preserved.

1 Table 1

2 Measurements (in mm) of RBINS M. 880 (cervical vertebrae) and M. 2280 (left humerus).

3 Characters are measured as preserved.

Character	Measure
M. 880 (cervical vertebrae)	
maximum anteroposterior length of whole complex	280
maximum transverse width of whole complex	423
maximum width across articular facets of atlas	384
maximum height of articular facets of atlas	175
posterior width of centrum of last cervical	246
posterior height of centrum of last cervical	201
M. 2280 (left humerus)	
total length	683
maximum proximal mediolateral width	355
maximum proximal anteroposterior width	458
anteroposterior diameter of humeral head	345
mediolateral diameter of humeral head	343
minimum mediolateral width of diaphysis	222
minimum anteroposterior width of diaphysis	271
distal mediolateral width	249
maximum distal anteroposterior width	364
anteroposterior length of radial facet	239
anteroposterior length of ulnar facet (including facet for olecranon)	250

Table 2 - Measurements (in mm) of the neurocranium RBINS M. 879a-f (holotype of *Eubalaena ianitrix* sp. nov.).

Characters are measured as preserved.

1 **Table 2**

2 Measurements (in mm) of the neurocranium RBINS M. 879a-f (holotype of *Eubalaena ianitrix*

3 sp. nov.). Characters are measured as preserved.

Character	Measure
bizygomatic width	1660
estimated postorbital width	1760
width of occipital condyles	290
distance between lateral margins of exoccipitals	850
length of supraoccipital shield from foramen magnum to vertex	560
height between basicranium and vertex	71
transverse width of maxillae at vertex	290